AUSTRALIAN SCIENCE & MATHEMATICS SCHOOL

International Science Fair 2008

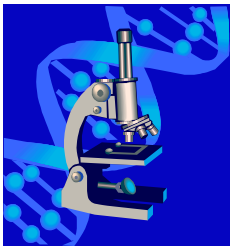

Student Research Journal

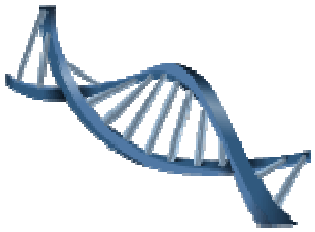

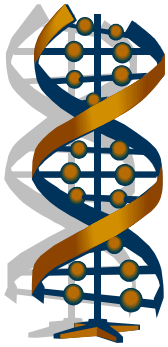

AUSTRALIAN SCIENCE & MATHEMATICS SCHOOL

Government of South Australia
Department of Education and Children's Services

Flinders University
Adelaide • Australia

The Australian Science and Mathematics School conducts an International Science Fair for invited students from partner schools on an annual basis. The students make an active contribution to the events of the science fair through presenting workshops and poster displays of aspects of the research work they undertake at their own schools.

In 2008 representative students have also presented formal written reports on their research work.

We are pleased to present these research reports in this *Student Research Journal* of the International Science Fair 2008.

Graeme Oliver
Event Director
ASMS International Science Fair
25th June 2008

Australian Science and Mathematics School
Flinders University
Sturt Road
BEDFORD PARK SA 5042
Telephone: +61 8 8201 5686
Facsimile: +61 8 8201 5685

Email: asms@flinders.edu.au
Website: http://www.asms.sa.edu.au

2008 Participating Schools

AUSTRALIAN SCIENCE AND MATHEMATICS SCHOOL

RITSUMEIKAN JUNIOR and SENIOR HIGH SCHOOL

MAHIDOL WITTAYANUSORN SCHOOL

COMO SECONDARY COLLEGE

MANITOBA LIFE SCIENCES PROJECT

KOREA SCIENCE ACADEMY

NATIONAL UNIVERSITY SINGAPORE HIGH SCHOOL

Principal's Introduction

Science is commonly defined as "knowledge attained through study or practice." It's really about a system of acquiring knowledge and it's a system that uses observation and experimentation to describe and explain natural phenomena. It's also often used as a term that refers to the organized body of knowledge people have gained using that system.

Science has always evolved through collaboration and scrutiny. The strength and integrity of our scientific knowledge comes about because science describes itself through investigation and inquiry. It is subject to test and re-test and to analysis, description and interpretation. And the purpose of science is to produce useful models of reality or to generate theoretical explanations of natural phenomena.

The rich and long history of science can be traced back to 3000 BC where the early civilizations of the Tigris-Euphrates valley and the Nile valley made advances in metallurgy, agriculture, transportation, navigation and calendar determination, all supported through the development of written language and mathematics. The search for answers continues today and modern science continues to grapple with many challenges. Energy supply and environmental sustainability immediately come to mind as do the fields of science, such as gene manipulation and organ transplantation that carry with them profound ethical considerations. Scientific activity finds itself inextricably placed within the political, economic, religious and social events and philosophies that shape our global communities of the 21st century.

The rigour of science is found through the interactions, collaborations, interpretations and replications generated by scientists around the world. The production of useful models of reality or the generation of theoretical explanations of natural phenomena rarely develop credibility and validity in the absence of the sharing of learning and understandings between scientists. When scientists write and talk about their scientific endeavour they immediately invite scrutiny, test, retest and replication. Another bit of knowledge is created and another scientist puzzles over new ideas and theorises and hypothesises about further new ideas.

Therein lays the importance of this publication. The generation of knowledge is not only in the hands of the experienced, professional research scientists. It also belongs to our young people who have the opportunity and interest in shaping their future through international collaboration and endeavour. The publication of their scientific activity is an important contribution to that future.

Associate Professor Jim Davies
Principal,
Australian Science & Mathematics School

Table of Contents

1. *Phoca hispida Feeding Ecology and Contaminant Uptake: Insights from Elemantal analyses of Claws* Page 5
   Author:Beth Ferreira-Manitoba life Sciences Project

2. *Effects of the Overexpressed Global Regulators in the Salmonella Pathogenesis* Page 10
   Author: Soo guen Shin, Hee-jin Son, Naye Choi –Korea Science Academy

3. *Towards the Design of a Stable DNA G-Quadruplex Structure* Page 15
   Author: Tan Zhong Ming—National University Singapore High School

4. *Phage Display Derived Human Monoclonal Antibody Binding to Nef Protein of HIV—1* Page 22
   Author: Jirapan Napapruekchart, Chanakarn Vipusmith, Nuthawadee Sae-Iah - Mahidol Wittayanusorn School

5. *Comparative Studies of Leaf Anatomy of Bougainvillea Sp* Page 25
   Author: Chanatip Chailek, Somruthai Homchuen—Mahidol Wittayanusorn School

6. *Detection and Typing of Dengue Viruses from Aedes sp. by Using One-Step reverse Transcriptase-Polymerase Chain Reaction* Page 27
   Author: Pichanon Mingchay, Supanan Sae-Lim—Mahidol Wittayanusorn School

7. *Bio-Stealth—Making Perfect Transparency* Page 29
   Author: Shun Yoshida—Ritsumeikan High School

8. *Biodiesel Renewable but Toxic* Page 32
   Author: Ross tieman, Ashleigh Fields—Australian Science and Mathematics School

9. *Design and Development of a Novel True Power Measurement Device* Page 34
   Author: Luke Victor—Australian Science and Mathematics School

10. *The Effect of Grey Water on Cherax Destructor* Page 36
    Author: James Galbraith, Laura Stradling - Australian Science and Mathematics School

11. *The Effects of Endophytic Actinobacteria Isolated from Lucerne Against fungal Root Diseases* Page 38
    Author: Courtney Mason -Australian Science and Mathematics School

Phoca hispida Feeding Ecology and Contaminant Uptake: Insights from Elemental Analyses of Claws

Beth Ferreira

Fort Richmond Collegiate
Winnipeg, Manitoba, Canada

Abstract

Phoca hispida (ringed seal) claws contain up to seven visible annular growth rings (*annuli*) that reflect a longer timeline of contaminant exposure compared to visceral tissue. This study assessed the potential of analyzing sections of *Phoca hispida* claws (n=12) to determine total mercury body burden in relation to muscle tissue. Mercury concentrations in the claws and muscle tissue were analyzed using cold vapor atomic absorption spectrometry (CVAAS). Stable isotopes of nitrogen ($^{15}N/^{14}N$) were determined using continuous flow ion mass spectroscopy (CFIR-MS). Positive linear relationships were detected between $\log_{10}$[Hg] in the base of the claws versus $\delta^{15}N$ values in muscle tissue; and $\delta^{15}N$ values in the base of the claws versus $\log_{10}$[Hg] in the muscle tissue. This study confirmed the use of claws as a tool in communicating overall mercury body burden in *Phoca hispida*.

---

1. Introduction

Phoca hispida (ringed seal) is the most abundant seal species in the Canadian Arctic. Its niche in the food web comprises of eating invertebrates such as *Themisto libellula* (amphipods), *Mysidacea* (mysids) and small fish such as *Boreogadus saida* (arctic cod), *Ammodytes hexaptera* (sand-lance), and *Mallotus villosus* (capelin) while serving as prey to *Ursus mamitus* (polar bear) and local Inuit. Mercury is a heavy metal neurotoxin that is released into the atmosphere by primarily anthropogenic sources (coal burning, industrial waste). The contaminant is deposited in the Arctic and circulated through the food web. Biomagni-fication is a process in which contaminants such as mercury travel up the food chain while increasing in concentration.

Exclusive stable isotope ratios are produced by autotrophs during the process of photosynthesis. Measure-ments of stable isotopes of nitrogen ($^{15}N/^{14}N$) can be traced to determine the components of specific Arctic food chains and have been recently developed to assess rates of contaminant biomagnification with respect to trophic level in Arctic organisms (Atwell et al., 1998; Campbell et al., 2005; Kelly, 2000).

2. Objective

Phoca hispida claws contain annuli (visible annular growth rings) that researchers have used to estimate an animal's age in the field as a supplement to teeth aging. Researchers have analyzed the entire claw for mercury (Freeman et al., 1973) but no previous studies have examined individual sections within the annuli for mercury. This study assessed the potential of analyzing annular sections of *Phoca hispida* claws to determine total mercury body burden in relation to muscle tissue.

3. Materials and Methods

3.1. Sample Collection

Local hunters harvested tissue and claw samples in fall of 2006. Sample sites included Arviat (n=7), a community on the East Coast of Hudson Bay and Sanikiluaq, (n=5), a community in the Belcher Islands in Western Hudson Bay. The Freshwater Institute Animal Care Committee approved sample collection protocol (FWI Animal Care Committee, 2006). All samples were harvested for studies conducted by other researchers affiliated with the Department of Fisheries and Oceans.

3.2. Sample Preparation and Analysis: CVAAS

Claws were boiled to remove excess skin and to loosen the nail bone, which was extracted manually using pliers. Claws were sectioned lengthwise using a wet saw. Individual claw sections were cut with a dremel along the annuli and weighed. Samples were digested in aqua regia (3HCl: $1HNO_3$) for two hours at 90^oC. Cold Vapour Atomic Absorption Spectrometry (CVAAS) was conducted to determine total mercury (THg) concentration. CVAAS apparatus consists of an autoinjector (Pulse Instrumentation), a peristaltic pump (Ismatec), a mercury monitor 3200 (Thermo-Separation Products), and a ChromJet Integrator (Thermo-Separation Products).

3.3. Sample Preparation and Analysis: CFIR-MS

Methodology for sample preparation was adapted from Folch et al. (1957). Claw and muscle tissues were freeze-dried and powdered upon sub-sampling. Sub-samples were then treated with a 2:1 chloroform: methanol solution to extract lipids, dried, then shipped to the University of Winnipeg Isotope Laboratory (UWIL) for analysis. Stable isotope analysis was conducted using continuous flow ion ratio mass spectroscopy (CFIR-MS). Data from CFIR-MS is expressed in delta values (δ) in units of parts per thousand differences (‰). Stable isotope ratios were calculated with respect to an international standard according to the formula:

$$\delta X = [(R_{sample}/R_{standard})-1] \times 1000$$

where δX is $\delta^{15}N$ and R is defined as the nitrogen ($^{15}N/^{14}N$) ratio.

4. Results

Total Hg in the claws ranged from 0.44-3.49µg/g in the tip (mean= 1.47µg/g), 0.49-8.92µg/g in the base (mean=3.89µg/g) and 0.44-12.54µg/g

in the entire claw (mean=2.48µg/g). Linear regressions confirmed a relationship between claw base section $\log_{10}$[Hg] versus muscle tissue $\log_{10}$[Hg] (r=0.8005, p=0.0018). $\delta^{15}N$ values ranged from 12.55-14.82‰ in muscle tissue (mean=14.10‰). $\log_{10}$[Hg] in the base of the claws versus $\log_{10}[\delta^{15}N]$ values in muscle showed a significant positive cor-relation (r=0.7569, p=0.0044) as well as muscle tissue $\log_{10}$[Hg] versus $\log_{10}[\delta^{15}N]$ values in the claw base section (r=0.7056, p=0.0099).

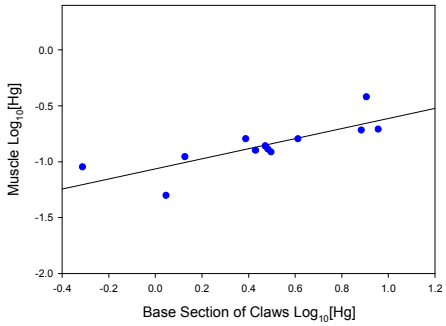

Figure 1. $\log_{10}$[Hg] in the muscle tissue versus $\log_{10}$[Hg] in the base section of claws (p<0.002)

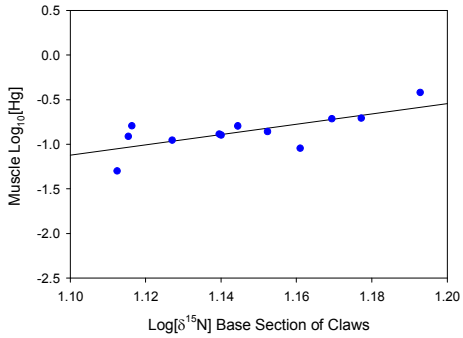

Figure 2. $Log_{10}[Hg]$ in the muscle tissue versus $log_{10}[\delta^{15}N]$ values in the base section of claws ($p<0.01$).

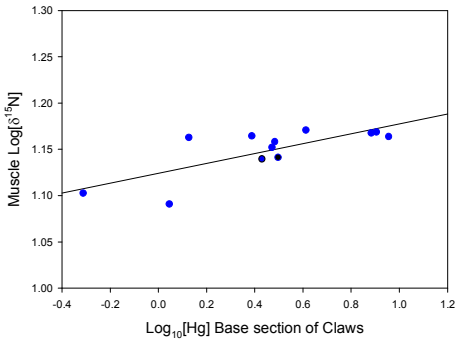

Figure 3. $Log_{10}[\delta^{15}N]$ values in muscle tissue versus $log_{10}[Hg]$ values in the base section of claws ($p<0.01$).

5. Conclusion

$\delta^{15}N$ enrichment occurs through the process of biomagnification. These $\delta^{15}N$ values in muscle tissue of *Phoca hispida* represent recent contaminant exposure. This study found significant positive relationships between $\delta^{15}N$ values and THg (total mercury) in the base of the claw versus THg and $\delta^{15}N$ values in the muscle tissue where base represents growth within the current year.

6. Application

This study confirmed the use of claws as a tool in communicating overall mercury body burden in *Phoca hispida*. Claws have the potential to reveal previous contaminant exposure through analysis of annular sections therefore assessing feeding ecology over a longer timeline than provided by analysis of visceral tissue.

7. Discussion

7.1. Alternative Tissue Analysis

Stable isotope and total mercury (THg) analyses were also conducted on the liver tissue. Muscle and liver tissue are both considered standards for THg analysis but THg values in the liver are less understood than THg values in the muscle tissue. The liver is considered a detoxifying organ and has a longer turnover rate than muscle tissue. Significant relationships were detected between THg in the liver versus THg in the base of the claws ($p<0.05$) and $\delta^{15}N$ values in the liver versus THg in the base of the claws ($p<0.05$). This study focused on relationships between claws and muscle tissue because mercury and $\delta^{15}N$ values in the liver tissue versus the claws reflected weaker relationships as compared to muscle tissue.

THg and $\delta^{15}N$ results in the claws were also compared to THg in the whiskers. Significant relationships were detected between THg in the base of the claws and THg in the whiskers ($p<0.01$) as well as $\delta^{15}N$ values in the base of the claws versus THg in the whiskers ($p<0.05$). Relationships between mercury values in the claws and whiskers suggest *Phoca hispida* may use all these tissues to store contaminants.

7.2. $\delta^{13}C$ Analysis

Stable isotopes of carbon ($^{13}C/^{12}C$) bioaccumulate in hetero-trophs leaving a distinct carbon signature that can be detected using continuous flow ion ratio mass spectroscopy. Carbon signatures indicate an organism's environment: benthic (near-shore) versus pelagic (offshore). $\delta^{13}C$ values were analyzed in the liver and muscle tissue as well as within the claw annular sections. $\delta^{13}C$ Signals suggested that pups in the Hudson Bay area fed near benthic sources on small invertebrates as opposed to adults who fed in pelagic regions on larger fish. Significant relationships were detected between $\delta^{13}C$ values in the base of the claws versus $\delta^{13}C$ values in muscle and liver tissues ($p<0.01$); $\delta^{13}C$ values in the base of the claws versus THg in muscle tissue ($p<0.01$); and $\delta^{13}C$ values in the base of the claws versus THg values in the base of the claws ($p<0.05$). These results suggest there is a relationship between environment and mercury body burden but further research is required to accurately trace the feeding ecology of *Phoca hispida* in the Hudson Bay area.

7.3. Comparison of Claw Annuli

This study analyzed individual annular sections of the claws for THg. THg values decreased along the length of the claw where the base had the highest THg values and the tip the lowest THg values. No significant relationships were detected between muscle tissue and the claws using the mean THg values for the entire length of the claw. All relationships between muscle tissue and claws used the THg value of the base section of the claw. The base represents the most recent year of contaminant exposure whereas the tip represents several years prior. The turnover rate of muscle tissue is under one year; therefore, they relate to the base of the claw. These results suggest that if the base is indicative of the mercury in the visceral tissue at present, previous sections of the claw are indicative of the mercury in the visceral tissue of past years.

7.4 Laser Ablation ICP-MS Analysis

Laser ablation inductively coupled plasma mass spectroscopy (LA-ICP-MS) was performed on a claw with 6 annular sections from an adult male. LA-ICP-MS has a low detection limit and was able to analyze the qualitative mercury trends throughout the entire length of the claw. These trends represented the changing of mercury concentrations over the last ~6 years of the animal's life. The mercury values seemed to fluctuate throughout the length of the claw. While LA-ICP-MS provided insights into the contaminant exposure history of the animal, the data was inconsistent and qualitative. More advances in the analytical technique are required in order to fully determine the quantitative changes of mercury concentration in *Phoca hispida* claws.

Acknowledgements

This project was completed under the co-operation and supervision of Fisheries and Oceans Canada. The following staff and students provided guidance and access to laboratories and samples: Lisa Loseto, Post Doctoral Fellow (Univ. of Victoria); Ashley Gade, M.Sc Candidate (Univ. of Manitoba); Tara Bortoluzzi, Ph.D Candidate (Univ. of Manitoba). Dr. Steven H. Ferguson, Research Scientist, Fisheries and Oceans Canada, was the project mentor.

The following organizations participated in the collection of the seal specimens and provided funding for Fisheries and Oceans Canada: University of Manitoba, Manitoba Hydro, Nunavut Implementation Fund, Nunavut Wildlife Management Board, ArcticNet, and hunters that co-operated through the Arviat and Sanikiluaq Hunters and Trappers Organization.

References

AMAP, 2005. AMAP Assessment 2002: Heavy Metals in the Arctic. Arctic monitoring and Assessment Programme (AMAP), Oslo, Norway, xvi + 265 pp.

Armstrong, F.A.J. and J.F. Uthe (1971). Semi-automated determination of mercury in animal tissue. Atomic Absorption Newsletter Vol. 10, No. 5: 101-103.

Atwell, L., Hobson, K.A., Welch, H.E., 1998. Biomagnification and bioaccumulation of mercury in an arctic marine food web: insights from stable nitrogen isotope analysis. Canadian Journal of Fish and Aquatic Science, 55:1114-1121.

Basu, N., Kwan, M. & Chan, H., 2006. Mercury but not organochlorines inhibits muscarinic cholinergic receptor binding in the cerebrum of ringed seals. Journal of Toxicology and Environmental Health, 69:1133-1143.

Bearhop, S., Furness, R.W., Hilton, G.M., Votier, S.C., Waldron, S., 2003. A forensic approach to understanding diet and habitat use from stable isotope analysis of (avian) claw material. Functional Ecology, 17: 270-275.

Bligh, E.G., Dyer, W.J., 1959. A rapid method of total lipid extration and purification. Canadian Journal of Biochemistry and Physiology 37: 911-917.

Campbell, L.M., Norstrom, R.J., Hobson, K.A., Muir, D.C.G., Backus, S., Fisk, A.T., 2005. Mercury and other trace elements in a pelagic Arctic marine food web (Northwater Polynya, Baffin Bay). Science of the Total Environment, 351-352: 247-263.

Dehn, L.A., Sheffield, G.G., Follmann, E.H., Duffy, L.K., Thomas, D.L., Bratton, G.R., Taylor, R.J., O'Hara, T.M., 2005. Trace elements in tissues of phocid seals harvested in the Alaskan and Canadian Arctic: influence of age and feeding ecology. Canadian Journal of Zoology, 83: 726-746.

Freshwater Institute Animal Care Committee (2006): Animal Use Protocol, Fisheries and Oceans Canada, Protocol number FWI-ACC-2006-2007-008.

Folch, J., Lees, M., Sloane Stanley, G.H., 1957. A simple method for the isolation and purification of total lipids from animal tissues. Journal of Biological Chemistry 226: 497-509.

Freeman, H. C., Horne, D.A., 1973. Mercury in Canadian Seals. Bulletin of Environmental Contamination & Toxicology 10:172-180.

Hobson, K.A., 1996. Stable carbon and nitrogen isotopic fractionation between diet and tissues of captive seals: implications for dietary reconstructions involving marine mammals. Canadian Journal of Fish and Aquatic Science, 53: 528-533.

Hobson, K.A., Schell, D.M., 1998. Stable carbon and nitrogen isotope patterns in baleen from eastern Arctic bowhead whales (*Balaena mysticetus*). Canadian Journal of Fish and Aquatic Science, 55: 2601-2607.

Hobson, K.A., Fisk, A., Karnovsky, N., Holst, M., Gagnon, J-M., Fortier, M., 2002. A stable isotope model for the North Water food web: implications for evaluating trophodynamics and the flow of energy and contaminants. Deep-Sea Research II, 49: 5131-5150.

Kelly, J.F., 2000. Stable isotopes of carbon and nitrogen in the study of avian and mammalian trophic ecology. Canadian Journal of Zoology, 78: 1-27.

Power, M., Klein, G.M., Guiguer, K.R.R.A., Kwan, M.K.H, 2002. Mercury accumulation in the fish community of a sub-Arctic lake in relation to trophic position and carbon sources. Journal of Applied Ecology, 39: 819-830.

Preston, T., 1992. The measurement of stable isotope natural abundance variations. Plant, Cell and Environment, 15: 1091-1097.

Ramsay, M.A., Hobson, K.A., 1991. Polar bears make little use of terrestrial food webs: evidence from stable-carbon isotope analysis. Oecologia 86: 598-600.

Smith, R.J., Hobson, K.A., Koopman, H.N., Lavigne, D.M., 1996. Distinguishing between populations of fresh and salt-water harbour seals (*Phoca vitulina*) using stable-isotope ratios and fatty acid profiles. Canadian Journal of Fish and Aquatic Science, 53: 272-279.

Wagemann, R., Trebacz, E., Boila, G., Lockhart, W.L., 1998. Methylmercury and total mercury in tissues of arctic marine mammals. Science of the Total Environment, 218: 19-31.

Zhao, L., Schell, D.M., 2004. Stable isotope ratios in harbor seal *Phoca vitulina* vibrissae: effects of growth patterns on ecological records. Marine Ecology Progress Series 281: 267-273.

Effects of the overexpressed global regulators in the *Salmonella* pathogenesis

Heejin Son[1], Naye Choi[1], Soogeun Shin[1], Mijin Oh[1], Seungmin Kim[1], Shinwook Park[1], Kwangil Kang[1], Hoyoung Kang[2], Ahyoung Yu[2], Jong Earn Yu[2]

Korea Science Academy(899, Danggam 3-Dong, Busanjin-Gu, Busan, South Korea)[1], Busan National University(30, Jangjeon-Dong, Geumjeong-gu, Busan, South Korea)[2]

I. Introduction

A. *Salmonella* and Salmonellosis

1) What is a *Salmonella*?

Salmonella is a genus of rod-shaped, Gram-negative bacteria belonging to the family of *Enterobacteriaceae*. *Salmonella* is classified according to serotype and differentiated by their habitats and antigenic characteristics. The genus *Salmonella* is divided into two species, *Salmonella enterica* and S. *bongori*. *Salmonella enterica* is further divided into six subspecies. There are also numerous (over 2500) serovars(serotypes) within both species, which are found in a disparate variety of environments and are associated with many different diseases.

2) What is a Salmonellosis?

Salmonellosis is the most common food-borne bacterial disease in the world. *Salmonella* can cause a systemic infection, gastroenteritis or septicaemic infections depending on the animal species and the host specificity of the infecting bacterial strain. There are two main clinical symptoms associated with *Salmonella*. Typhoid fever caused by *S. typhi* or *S*. *paratyphi* is characterized by protracted bacteremia but minimal gastrointestinal symptoms. The nontyphoidal *Salmonella* results in symptoms including diarrhea, vomiting abdominal cramps and fever.

3) How does *Salmonella* infect and escape from host defense?

Salmonella usually infects animals and humans by the oral route with contaminated food or water. During infection, *Salmonella* resists the defense system of the host. *Salmonella* could migrate from the gastrointestinal tract to the bloodstream through mesenteric lymph nodes and lymphatic vessels. During the *Salmonella* pathogenesis process, a number of virulence determinants are required for the invasion and survival in the intracellular compartment. Because the expression of many virulence determinants are regulated by so-called global regulator, examination of the function of global regulator considered to important in the understanding of *Salmonella* mediated pathogenesis. In this research we conducted experiments to determine *Salmonella* virulence with strains overexpressing global regulators.

B. Selected virulence factors of our research.

1) Lon

Lon is a homo-oligomeric ATP dependent protease localized in the cytosol of prokaryotes. Its primary function is to degrade the denatured, oxidatively damaged and certain regulatory proteins in the cell. After recognition and binding of the substrate to the Lon, hydrolysis of ATP permits substrate unfolding; the unfolded substrate is then translocated into the proteolytic chamber of the Lon where processive peptide bond cleavage takes place. The *Salmonella* strain lacking Lon attenuates virulence in mouse model.

2) OmpR

OmpR regulates the porin genes *ompF* and *ompC* in response to osmolarity changes. At low osmolarity, OmpR activates the expression of OmpF . At high osmolarity, OmpR–OmpR interactions stimulate formation of a loop that represses *ompF*. In addition to osmolarity regulation OmpR regulates the expression of other virulence factors including adhesions and acid tolerance *etc*. The *Salmonella* strain lacking OmpR attenuates virulence in mouse model.

3) Crp (cyclic AMP receptor protein)

Crp plays an important role in regulating the metabolism of carbohydrates in prokaryotes. Crp conformation and activity as a transcription factor are dependent upon cAMP. In the presence of cAMP, Crp changes a conformation that promotes its interaction with DNA and RNA polymerase (RNAP). These interactions are the essential step to establishing active transcription complexes on the CRP-dependent promoters. The *Salmonella* strain lacking Crp attenuates virulence completely in mouse model.

2. Materials and Methods

A. Bacterial strains, plasmids and culture conditions

Various *Salmonella typhimurium mutants*, Δ*lon*, Δ*ompR* and Δ*crp,* were used in virulence studies. *Escherichia coli* strains were used for cloning host. All bacterial strains were grown at 37□ in Luria-Bertani (LB) broth or LB (3). Ampicillin, when required, is added in the culture medium with the 100 μg/ml concentration. Diaminopimelic acid (DAP) was added (50 μg/ml) for the Asd^- strains.

B. General DNA manipulation

DNA manipulations were carried out as described by Sambrook *et al* (5). Transformation of *E. coli* and *Salmonella* were done with either rubidium chloride-heat shock or electroporation (BioRad). PCR amplification was employed to obtain DNA fragments for cloning. The PCR conditions were as follows: denaturation at 95□ for 30 sec, primer annealing at 50~55□ according to melting temperature of primers for 30 sec, polymerization at 72□ for 1~2 min, depending on the length of DNA fragment, and final extension at 72□ for 10 min.

C. SDS-PAGE

Protein samples prepared with lysis buffer were boiled for 5 min and then separated by discontinuous sodium dodecyl sulfate-polyacrylamide gel electrophoresis (SDS-PAGE). Proteins were visualized by Coomassie brilliant blue staining.

D. Immunoblot analysis

For immunoblotting, proteins separated by SDS-PAGE were transferred to nitrocellulose membrane in Towbin's Buffer. The membranes were blocked with 5% skim milk in Towbin's Saline Buffer for 3 hr as described by Towbin *et al* (6). The membrane was incubated with suitably diluted rabbit or mouse antisera in 5% skim milk for 2 hr and followed by 1:2000 dilutions of a horseradish peroxidase conjugated goat anti-rabbit IgG (H+L) in skim milk. Immunoreactive bands were detected by the addition of 4-chloro-1-naphthol in the presence of hydrogen peroxide. The reaction was stopped after 5 min by washing with several changes of large volume of deionized water.

III. Result and discussion

A. Schematic presentation of overall experiment processes

B. Construction of recombinant plasmids for overexpression of target protein

Target DNA was obtained by PCR amplification using appropriate primer set from *Salmonella* chromosomal DNA. Each primer was designed according to complete ORF of each gene (Table 1). DNA fragments shown proper size were confirmed by agarose gel electrophoresis (data not shown). All PCR products were subcloned into pGEM T-vector, resulting in pBP548(*crp*) and pBP566(*ompR*). DNA fragments cut by restriction enzyme were transferred to pYA3342 expression vector that has *asd* gene for selection marker, resulting in pBP570(*ompR*), pBP571(*crp*). PCR products of *lon* were directly ligated to pYA3342 and designated as pBP572 (data not shown). Each recombinant plasmid was transferred to *Salmonella* strain.

Number	Primer Name	Oligonucleotide sequence	Characteristics
1	Crp-F(EcoRI)	5'-gaattcgcatggtgcttggcaaa-3'	PCR for crp
2	Crp-R(HindIII)	5'-gcaagcttttaacgggtgccgta-3'	PCR for crp
3	OmpR-F(NcoI)	5'-ccatggaagagaattataagatt-3'	PCR for ompR
4	OmpR-R(HindIII)	5'-gcaagctttcatgctttagaacc-3'	PCR for ompR
5	Lon-F(NcoI)	5'-ccatggatcctgagcgttctgaac-3'	PCR for lon
6	Lon-R(HindIII)	5'-gcaagcttctattttgcggttac-3'	PCR for lon

Table1] Primers used in the experiment

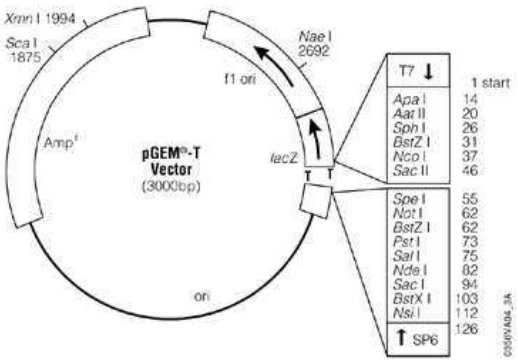

[Figure1] vector map of pGEM-Tvector

C. Confirmation of the overexpression of target proteins in cells containing recombinant plasmids

Using target protein-specific antibody, we confirmed the recombinant plasmid-derived overexpressed protein in each *Salmonella* stains. We could show that each target protein was overexpressed in *Salmonella* as compared with the wild-type.

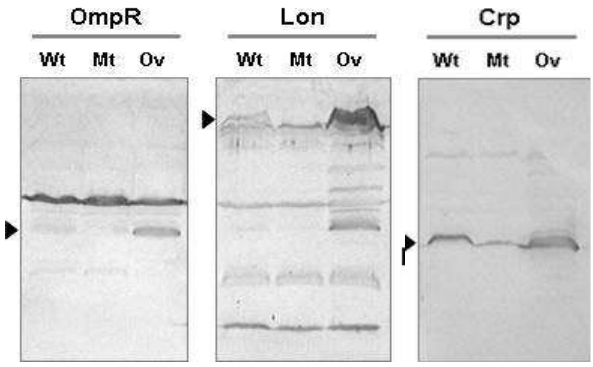

[Figure2] Western-blot analysis of OmpR, Lon, Crp
Wt : wild type *Salmonella* Mt: mutant *Salmonella*
Ov: overespressed *Salmonella*

D. Effect of *Salmonella* strains overexpressing regulator in the animals

Salmonella strains with confirmed overexpressed protein was injected to the host(mice)(Table2) after counting using viable test and OD_{600}. Although it was expected that the injected mice would show some sort of sickness, all of them survived without specific symptoms. It is not sure that the dose we employed is adequate for our purpose. We think the dose we applied is little low to accomplish our proposed experiments. Since animal experiments need to be of repeated in order to be valued, it is required to perform the experiment again to get valuable results for this research,

***Salmonella* strain**	**Number of injected *Salmonella*(CFU/20 μl)**
wild-type	1.82×10^4
χ8554/pYA3342::ompR	1.60×10^4
χ8554/pYA3342::lon	1.42×10^4
χ8554/pYA3342::crp	4.44×10^3

[Table2] Numbers of injected *Salmonella*

□. References

1. **Farmer, J. J.** 1995. Enterobacteriaceae: introduction and identification, p.438-449. In Murray, P. R., E. J. Baron, and M.A. Pfaller (ed.). Manual of clinical microbiology, 6th ed. American Society for Microbiology, Washington, D. C.

2. **Chiu, C. H., L. H. Su, and C. Chu.** 2004. *Salmonella enterica* Serotype Choleraesuis: Epidemiology, Pathogenesis, Clinical Disease, and Treatement. Clinical Microbiology Reviews. **17:**197-202.

3. **Bertani, G.** 1951. Sudies on lysogenesis. I. The mode of phage liberation by lysogenic *Escherichia coli*. J. Bacteriol. **62:**293-300.

4. **Nakayama K., S. M. Kelly, and R. Curtiss III.** 1988. Construction of an ASD^+ expression -cloning vector: stable maintenance and high level expression of cloned genes in a Salmonella vaccine strain. Biotechnol. **6:**693-697.

5. **Sambrook, J, and D. W. Russel.** 2001. Molecular cloning a laboratory manual, 3rd ed. Cold Spring Harbor Laboratory Press. Cold Spring Harbor, N.Y.

6. **Towbin, H., T. Staegelin, and J. Gordon.** 1979. Electophoretic transfer of proteins from polyacrylamide gels to nitrocellulose sheets: procedure and some applications. Proc Natl Acad Sci. USA. **76:**4350-54.

Towards the design of a stable DNA G-quadruplex Structure

Tan Zhong Ming
NUS High School of Math and Science

Ang Wan Lin Rita
River Valley High School

Supervisor:
Assistant Professor Phan Anh Tuan
Division of Physics and Applied Physics, School of Physical and Mathematical Sciences, Nanyang Technological University

ABSTRACT

DNA as established by the Watson-Crick duo adopts the Watson-Crick double helix structure. However, other lesser-known structures could be formed, one of them being the G-quadruplex structure formed by Guanine–rich sequences that conform to tetrads of hydrogen-bonded guanine bases. Three-layer G-quadruplexes are widely described in literature, with the human telomere sequence. This project aims to understand the structures of G-quadruplexes of different number of layers (2 and 4). This work involved preparation of oligonucleotides and analysis of their structures by Nuclear Magnetic Resonance (NMR) spectrometry and Circular Dichroism (CD). Our research has found that the *Bombyx Mori* folds into a 2 layer G-quadruplex structure. This quadruplex contains 4 *syn* guanines and 4 *anti* guanines, involving a global anti-parallel conformation. All these results together prompted us to propose 3 possible models.

Keywords: DNA, Quadruplex, Guanine, *Bombyx Mori, Cryptococcus*

INTRODUCTION

I. DNA and G-Quadruplex Structure

Deoxyribonucleic acid (DNA), the genetic material of all living organisms, is a polymer made up of permutations based on the four nucleotides (Adenine, Thymine, Guanine and Cytosine). This material is mainly organised into a double helix conformation as described in the Watson-Crick model. This canonical structure, however, is not the only structure DNA can conform to. In fact, DNA is prone to structural polymorphism: besides this famous double helix, other more complicated structures may be formed. G-quadruplexes (G4) constitute an example of such unusual nucleic acids structures. This higher-order DNA structure, is formed from guanine-rich DNA sequences containing 4 blocks of guanines separated by 1 to 9 nucleotides. They result from the stacking of several quartets; each quartet being a planar association of four guanines held together by 8 hydrogen bonds and stabilized by monovalent Na^+ and K^+ cations *(Fig. 1a)* [1]. The intramolecular G4 structure is able to loop in different ways *(Fig. 1b)*, based on the respective conditions subjected to. This folding relies on numerous parameters such as the sequence, the nature and the concentration of the cation (K+ or Na+) and the pH.

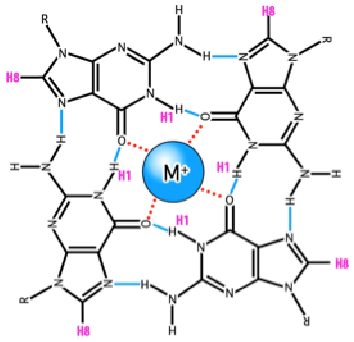

Fig 1a. The guanines are Hoogsten-hydrogen bonded (blue), and stabilized by a monovalent cation M^+(red). [6] H1 and H8 are labeled in the above diagram

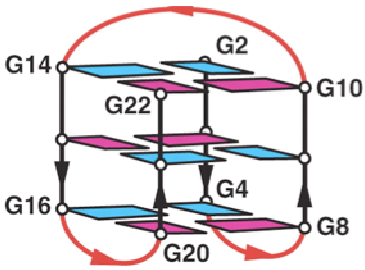

Fig 1b. NMR-based folding topology of d [TAGG(TTAGGG)$_3$ in Na^+ solution[8]

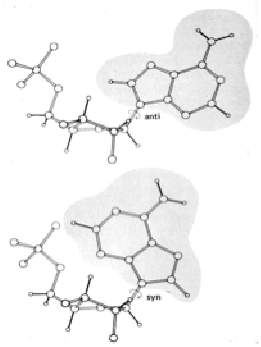

Fig 1c. The guanines, with their sugar bases and phosphate backbones. (Top) Guanine in *anti*-conformation. (Bottom) Guanine in *syn*-conformation. [7]

The telomeric G4 represented in *Figure 1b* and *Figure 1d* consists of three G-tetrads linked with mixed parallel–antiparallel G-strands. This folding is a direct consequence of the precise alternation of *syn* and *anti* guanine conformation *(Fig. 1c)*. This sequence adopts a folding called 'basket'. It is composed of 2 TTA edgewise loops (the 1st and the 3rd) and one TTA diagonal loop (the 2nd) [2]. 3 other folding have also been described: the chair conformation, the (3+1) and the parallel [3]. Thus, G-quadruplex structures of DNA are highly adaptable to form different conformations.

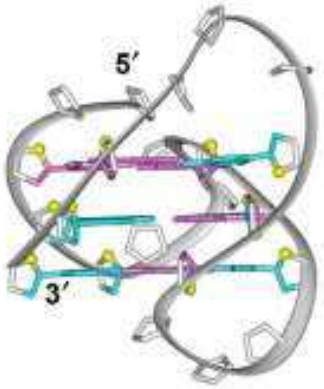

Fig. 1d Ribbon view of natural human telomere sequence (Fig 1c.) d[TAGGG(TTAGGG)$_3$. [8]

II. G4 Biological Properties

One of the most famous G-rich sequences is found in a 3' overhang located at the ends of chromosomes, called telomeres. This 3' overhang is composed of the following repeated motif: $(T_2AG_3)_n$, which is able to form G4 structures. When chromosomes are replicated, the DNA polymerase complex is unable to replicate this overhang, resulting in a shortening of the telomeres at each division. In normal sequences, when a critical minimal length is reached, the cell is programmed to die. The protein telomerase is active in cancer cells while almost absent in all other cells. The consequence is that the life of the cancerous cell is elongated, by regenerating the telomere overhang [4]. Therefore, Telomeres and telomerase represent, at least in theory, attractive targets for cancer therapy [5]. Stabilising the G4 structure located at the 3' G-rich telomeric overhang, by using small chemical compounds, could block telomerase activity.

III. Our Research

Our research deals with the design of a stable G-quadruplex structure of DNA, through experiments conducted using telomeric sequences of 2 eukaryotic organisms: the larva of the domesticated silkworm, *Bombyx mori* (telomere repeat, T_2AG_2) and the fungus *Cryptococcus* (telomere repeat, T_2AG_4). *Bombyx Mori* (*Bm)* sequence can form a two layer G4 *(Table 1)* while *Cryptococcus (C)* can form a four layer G4, as opposed to the human telomeric sequence that forms a three layer G4 *(Fig. 1b)*. *C* sequence forms multiple structures of 4 layers and was difficult to manipulate and solve. Therefore, the scope of the project was eventually narrowed to focus only on the *Bm* sequence. The results to the sequence will be discussed further in the following pages. Through studying the various tetraplex layers and using the methods of synthesis and nuclear magnetic resonance, we aim to be able to obtain a relationship between the number of layers and the looping conformation of the G4.

MATERIALS AND METHODOLOGY

I. Oligonucleotide Synthesis: General Procedures

Unlabeled and site-specific low-enrichment (1.5% ^{15}N-labelled) oligonucleotides were synthesized on an ABI 394 DNA synthesizer, deprotected with ammonium hydroxide, purified using a purification cartridge and finally dialysed in both water and 50mM KCL solutions. Concentration of the oligo was determined by UV and was around 0.1mM in 500µl. The whole protocol from the synthesis to the obtaining of the oligo NMR sample will take at least 3 days to complete.

II. NMR Spectroscopy

All experiments were conducted on a 600MHz Bruker spectrophotometer. Two kinds of NMR experiments were used: the 1-dimensional (1D) and the 2-dimensional (2D). The 1D experiments, as shown in Figure 3, are performed in H_2O and allow us to count the H1 imino protons (*Fig. 1a*) involved in the tetrads as well as to check the quality of the spectra, which are associated with the number of structures adopted by the DNA sequences. The 2D experiments, on the other hand, were conducted using Nuclear Overhausen effect spectroscopy (NOESY), in D_2O and then in H_2O, with each experiment lasting for about 12 hours, depending on the concentration of the sample. The experiment in D_2O serves to determine the composition of each tetrad. In fact, we can observe the through space interaction between the H1 and H8 of 2 different guanines belonging to the same tetrad. The H_2O 2D experiments, will allow us to determine the number of guanines in *syn* conformation (*Fig. 1c*) involved in the G4.

The NMR experiments were carried out at the standard conditions: 298 K, a 70mM KCl and 20 mM phosphate buffer at pH 7. These conditions were derived after testing *Bm* sequences under various conditions, such as setting the temperature from 278K—313K, K+ concentration from 20mM—100mM, all of which did not produce much difference from the original conditions.

III. Circular Dichroism Spectroscopy

Circular Dichroism is based on the differential absorption of left- and right-handed circularly polarized light and was used to determine the general conformation of the tetrads (whether the strands connecting are running parallel or anti-parallel).

RESULTS AND DISCUSSION

I. Peaks Show More Than One Conformation

Fig. 2 represents the 1D spectrum of *Bm1*. The region of 10-13 ppm is specific to the imino H1 protons, which are involved in hydrogen bonding. Therefore, each G4 tetrad presents 4 H1 protons. The number of peaks in this region involved in the G4 corresponds to the number of tetrad layers. Eight distinct peaks were predicted for *Bm1,* assuming there was only one species. Results have shown to be around double of our predicted values, with tendency the remaining of the peaks overlapping on a 1D test (the peaks are marked as in *Fig. 2*). These results show that *Bm1* sequence adopts 2 different folding in almost the same proportion (50% each). As it is difficult to study two different folds of similar concentration at one time, the goal of the project then became separating the species and studying them individually. To do so, factors had to be manipulated to favour one species.

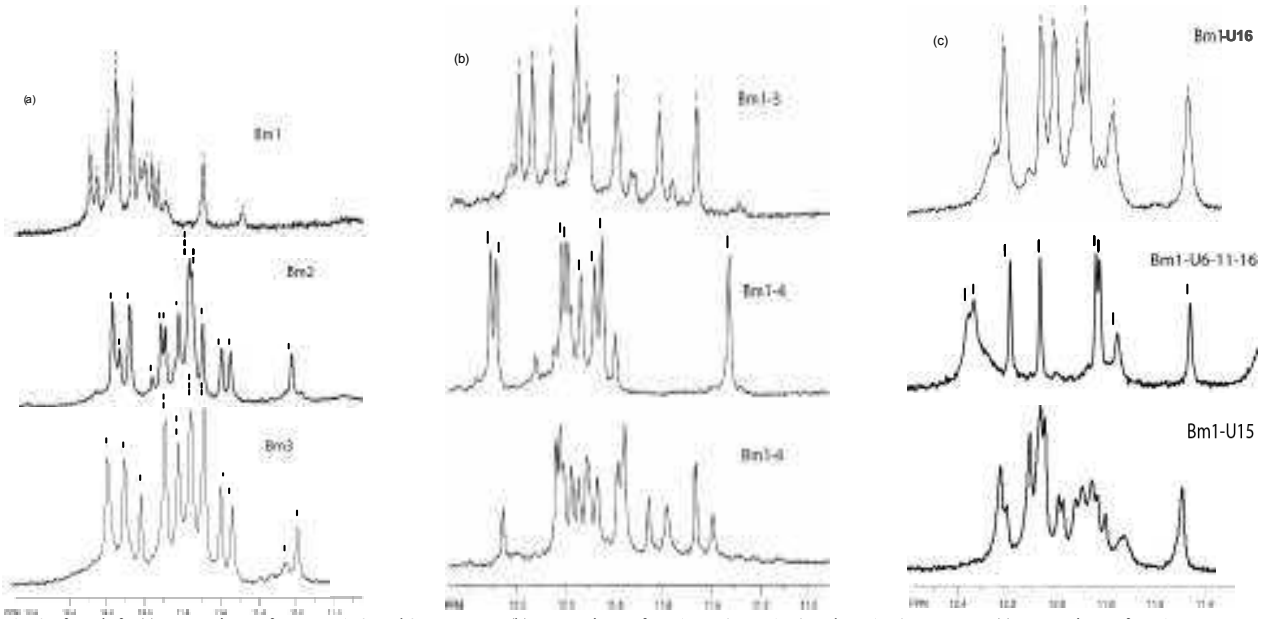

Fig. 2 , from left: (a) comparison of Bm 1, 2 and 3 spectrums (b) comparison of Bm1 -3, Bm1 -4 and Bm1 -6 spectrums (c) comparison of Bm1 -U16, Bm1 -U6-11-16 and Bm1 -U15. From the above spectrums, the difference between good spect rums which give differentiation of the 2 species present can be seen. In Bm1 -6 and Bm1 -U15, no differentiation could be seen.

II. Favouring One Species:

2 different strategies were used to favour 1 species over the other.

A. Modification to the Ends of Sequences and Their Effects

Modifications of sequences have yielded viable results with the human three-layer sequence, and hence we intended to test the viability of a modified sequence for *Bm1*, with the modifications shown in *Table 1(for Bm2 and Bm3)*. However, experiment results have shown otherwise. From *Fig. 2*, these modified sequences did not result in a single species dominating the solution with 8 very clear distinct peaks. It should be noted that the modification of a sequence is of much lesser biological relevance than the original sequence. Hence, we kept working with the *Bm1* sequence.

Table 1: Modifications to the ends of sequences

Bm1	TAGGTTAGGTTAGGTTAGG
Bm2	TTGGTTAGGTTAGGTTAGGA
Bm3	TTGGTTAGGTTAGGTTAGGAA

B. Modifications of Certain Bases Within Sequences and Their Effects

In this strategy, a normal guanine was replaced by a bromo-guanine (BrG) (shown in *Fig. 3* in comparison with guanine) during the synthesis process at different locations of the sequence, effectively forcing the designated guanines to *syn*
conformation. The modifications are shown in *Table 2*. The results shown in *Fig. 2b* improved dramatically. The best results for *Bm1* yield from the substitution of the third and fourth guanine in *Bm1-3 and Bm1-4*, resulting in an almost total dominance of a single species (the major peaks belonging to the same species have been marked). In contrary, for the *Bm1-6,*16 peaks of the same intensity can be seen and the modifications yielded less interesting results *(Fig. 3a)*. A bromo-guanine can only adopt a *syn* conformation. This conformation is also only compatible with an anti-parallel G4 structure. Thus, it is conclusive that Bm1-3 and 4 are anti parallel G4.

Table 2: Bromo-guanine modifications made

Bm 1-1	TABrGGTTAGGTTA GGTTAGG	Bm 1-2	TAGBrGTTAGGTTA GGTTAGG
Bm 1-3	TAGGTTABrGGTTA GGTTAGG	Bm 1-4	TAGGTTAGBrGTTA GGTTAGG
Bm 1-5	TAGGTTAGGTTABr GGTTAGG	Bm 1-6	TAGGTTAGGTTAGB rGTTAGG
Bm 1-7	TAGGTTAGGTTAGG TTABrGG	Bm 1-8	TAGGTTAGGTTAG GTTAGBrG

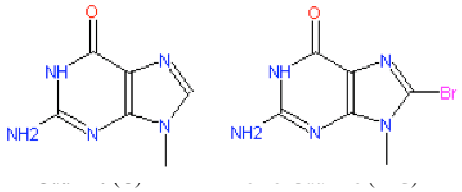

Fig. 3 Above: Left is a normal guanine and right is a bromo-guanine; Below: left is a uracil base and right is a thymine base.

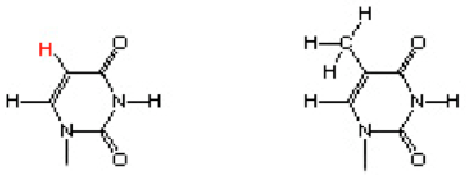

Uracil (U) Thymine

An interesting result was also obtained using the T to U substitution (*Fig. 2c*, Table 3).

Table 3: Modifications using Uracil

Bm1-U1	UAGGTTAGGTTAGGTTAGG	Bm1-U5	TAGGUTAGGTTAGGTTAGG
Bm1-U6	TAGGTUAGGTTAGGTTAGG	Bm1-U10	TAGGTTAGGUTAGGTTAGG
Bm1-U11	TAGGTTAGGTUAGGTTAGG	Bm1-U15	TAGGTTAGGTTAGGUTAGG
Bm1-U16	TAGGTTAGGTTAGGTUAGG	Bm1-U11-16	TAGGTTAGGTUAGGTUAGG
Bm1-U6-11-16	TAGGTUAGGTUAGGTUAGG		

For *Bm1-U16* and *Bm1-U6-11-16*, 8 major peaks can be easily counted, in contrary to *Bm1-U15* where an equal mix of 2 folds is still present. The same spectrum quality was obtained for *Bm1-U16* and *Bm1-U6-11-16.* We focused on *Bm1-U16* which contained only one substitution. We now have 3 interesting sequences: *Bm1-3*, *Bm1-4* and *Bm1-U16*, that will allow us to identify the two different folds in equilibrium in the case of *Bm1* wild type sequence.

III. Strands Holding Tetrads Run Anti-Parallel

In *Fig. 4*, the positive peak at 294 and the negative peak at 270 nm indicate that for *Bm1*, *Bm1-3* and *Bm1-4*, the strand runs anti parallel, as suggested by Balagurumoorthy and Brahmachari [9].

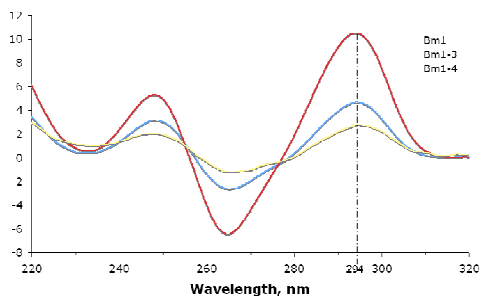

Fig. 4 Circular Dichroism Spectrum

IV. Identification of the 2 Forms By 2D NMR

Upon narrowing down all possibilities and isolating a single species through favouring, we have deduced that Bm1, $TAGG(TTAGG)_3$, consists of 2 forms, in a 1:1 ratio. As such, through further modifications, it was hypothesized that *Bm1-3* and *Bm1-U16* each consists of a separate dominant species. In addition, after further analysis, it was found that *Bm1-4* shares a common peak with *Bm1-U16* at the extreme ends of the spectrum (*Fig. 2*). Thus, Bm1-4 should contain the same folding topology as that of Bm1-U16. Due to this hypothesis, the focus of our work was shifted to focus on Bm1-3 and Bm1-U16.

In order to identify the number of *syn* guanine, 2D NOESY 300ms in D_2O was performed. The intensity of the NOE signal between H1' (located in the sugar) and H8 (located at the guanine of the same nucleotide) is stronger in the *syn* conformation than in the *anti*. This is linked to the shorter distance between the 2 protons when in *syn* conformation (*Fig. 1c*). In *Fig. 5*, *Bm1-U16* presents 4 strong peaks due to the presence of 4 guanines adopting a *syn* conformation.

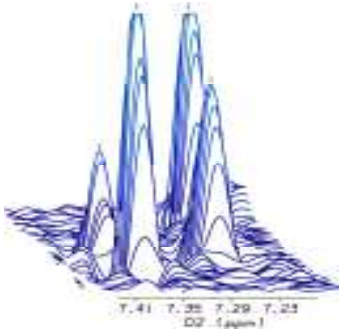

Fig. 5 The NOESY spectrum has been reduced to 7.23-7.41 ppm because the intensity of the interaction is shown only within this short r egion.

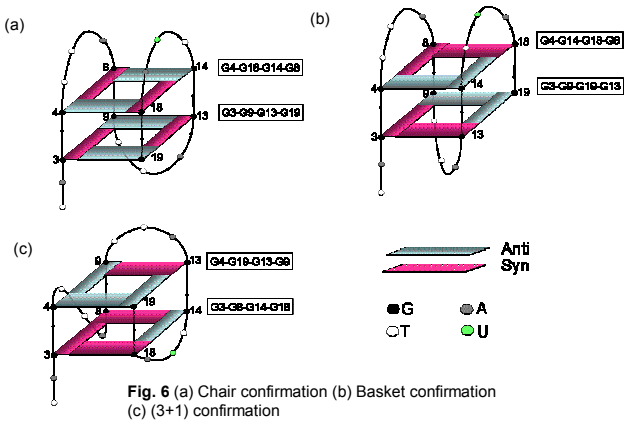

Fig. 6 (a) Chair confirmation (b) Basket confirmation (c) (3+1) confirmation

V. Hypothesized Folding of the *Bombyx mori* Structure

From the determination of four *syn*-conformation guanines, several foldings are hypothesized. The *syn* conformation indicates to us that the strands run anti-parallel, and hence, there must be a change in direction of the loops, a bend that will allow one *syn*-guanine to bond into the G4-tetrad. The plausible folding structures are: chair *(Fig. 6a)*, basket *(Fig. 6b)*, and the (3+1) conformation *(Fig. 6c)*. The chair conformation involves the G4-G18*-G14-G8* (asterik indicating *syn* conformation) on one layer while G3*-G9-G13*-G19 on another layer. The basket conformation also involves the same guanines but in a different order: G4-G14-G18*-G8* for the top end and G3-G13-G19-G9 for the bottom. In the case of the (3+1), the quartets have a different composition: top: G3*-G9-G19-G13* and bottom: G3*-G8*-G14-G18*. In the chair conformation, 3 edge wise loops are found. For the basket, we have 2 edgewise and 1 diagonal, and finally in the (3+1), a single double chain reversal loop and 2 edgewise loops can be found.

To identify which of the 3 foldings is adopted by Bm1-U16, there is a need to identify the guanine composition of each tetrad and the neighbouring guanine of each G. This will be done soon by performing a 2D NOESY 300ms experiment in H_2O. This will allow us to see the interaction between H1 and H8 of 2 guanines of the same tetrad.

VI. Determination of major folding of *Bombyx Mori* by ^{15}N assignment

Site-specific low-enrichment (1.5%) ^{15}N, isotope-labelling methods to assign unambigiuously all of the guanine imino protons. Natural abundance of ^{15}N is 0.37%, and an increase in abundance is recognised by the NMR experiment run. Multiple sequences were synthesised with each ^{15}N guanine assigned to one position. Through such assignment, individual guanines and their NMR peaks can be characterized, by individual 1D experiments.

The assignment of peaks of specific guanine imino protons allowed further analysis of the 2D NOESY 300 ms experiment ran previously. Intra-planar connectivity between different guanines (*Fig. 7)* showed that the two tetraplex formed with a structural composition of G4-G14-G18*-G8* for the top layer and G3-G13-G19-G9 for the bottom. This result shows that the major fold of *Bm1-U16* is the basket conformation.

CONCLUSION

The field of DNA research applications is ever changing and diverse. It is a field that will have much impact on future medical researches, especially in the field of cancer studies. In our research, we have successfully hypothesized 3 different possible conformations that the *Bombyx Mori* sequence is able to take, through both 1D and 2D NMR methods, and determined the major fold as the basket conformation. We believe that our research will become a stepping-stone for future researchers to study the second fold of *Bm1*, the folding topology in *C*, as well as the effects of looping.

ACKNOWLEDGEMENTS

Our sincerest gratitude goes out to the following people:

Our supervisor A/P Phan Anh Tuan, School of Physical & Mathematical Sciences, for his guidance.

Dr Samir Amrane, School of Physical & Mathematical Sciences, for his help and teachings of the subject.

Joefina and Jocelyn, for helping us familiarise ourselves with laboratory equipments when we were starting out.

The entire team at the School of Physical & Mathematical Sciences Biophysics lab, who have aided us in one way or another.

REFERENCES

[1]Gellert M, Lipsett MN, Davies DR (1962) Helix formation by guanylic acid. *Proc. Natl Acad. Sci. USA*, **48**, 2013–2018.

[2]Wang Y, Patel DJ (1993) Solution structure of a parallel-stranded G-quadruplex DNA. J Mol Biol., **234**, 1171-1183.

[3]Phan, AT, Luu, KN, Patel, DJ (2006) Different loop arrangements of intramolecular human telomeric (3+1) G-quadruplexes in K+ solution. Nucleic Acids Res., **34,** 19, 5715-5719.

[4]Maizels, N (2006) Dynamic roles for G4 DNA in the biology of eukaryotic cells. *Nat. stuct.* **13**, 12, 1055-1059.

[5]Dahse R, Fiedler W, Ernst G (1997) Telomeres and telomerase: biological and clinical importance [Review]. *Clin Chem* 43:708-714.

[6]http://upload.wikimedia.org/wikipedia/en/c/c1/G-quadruplex.gif

[7]http://nar.oxfordjournals.org/cgi/content/full/gkm706v2

[8]http://cmgm.stanford.edu/biochem201/Slides/DNA%20Structure/010%20Anti%20vs%20Syn%20Conform.JPG

[9]Balagurumoorthy P, Brahmachari SK. (1994) Structure and stability of human telomeric sequence. *J. Biol. Chem.*, **269**, 21858-21869.

Phage display derived human monoclonal antibody binding to Nef protein of HIV-1

Chanakarn Vipusmith[1] , Jirapan Napapruakchart[1] , Nutthawadee Sae-Iah[1] , Supanan Sae-Lim[1] , Sukanya Kwangsri[2] , Jenjira Saelim[2] , Anchalee Tungtronchitr[2], Kovit Pattanapanyasart[2] , Wanpen Chaicumpa[2] , Nitat Sookrung[2]
1 Mahidol Wittayanusorn school, Bangkok 73170, Thailand
2 Faculty of Medicine Siriraj Hospital, Mahidol University, Bangkok 10700, Thailand

Abstract

HIV-1 virus is the cause of AIDS (Acquired Immune Deficiency Syndrome), an important worldwide pandemic. HIV-1 virus has many proteins and among them Nef plays an important role in accelerating endocytosis and subsequenting degradation of CD4, MHC class I and II molecules on the cell surface. The purpose of this study to select phage expressing scFv specifically to Nef protein using bio-panning to test the binding between phage expressing scFv and Nef protein. The phages expressing scFv were cultured in *E.coli* cells and picked up as samples which were tested for the existence of phage by PCR. To test the pattern of the scFv molecule genes, Restriction Fragment Length Polymorphism (RFLP) was used in this process and ELISA was used next to test the specifically between phage expressing scFv and Nef protein. According to the result from all experiments, there were 1,367 *E.coli* colonies in 3 plates, and among 60 colonies there were 12 (20%) colonies having phage. All of the 12 colonies expressed different scFv phages having higher optical density (OD) than the negative controls, blanked by coating buffer. Among the selected colonies, 4 clones have optical density about two times higher than the blank. For the future study, these scFv will be tested for Nef protein inhibiting efficiency for developing immunotherapy.

Introduction

HIV-1 virus is the cause of AIDS (Acquired Immune Deficiency Syndrome), an important worldwide pandemic. HIV-1 virus has many proteins and among them Nef plays an important role in accelerating endocytosis and subsequenting degradation of CD4, MHC class I and II molecules on the cell surface.

Objective

1. To select human monoclonal antibodies ScFv (single chain variable fragment) which are specific for Nef protein of HIV-1 virus from antibody phage library.
2. To learn and practice about laboratory skills in molecular immunology.

Materials and Methods

1. Phage bio-panning for selecting phage clones that display HuScFv specific to the recombinant Nef proteinPhage library displaying human single chain variable fragment.

The M13 phage library displaying human single chain variable fragments (VH-peptide linker-VL; HuScFv) was constructed in Prof. Wanpen Chaicumpa laboratory from peripheral blood B lymphocytes of 60 Thai blood donors. This large repertoire library had an antibody diversity of ~2.6 x 108.

2. Preparation of E.coli transformants carrying recombinant huscFv-phagemids

Purified recombinant Nef protein was used as antigens in phage bio-panning to select phage clones displaying HuScFv that could bind to the protein. In the bio-panning process, one microgram of purified recombinant protein was individually immobilized in well of an ELISA plate. The plate was incubated at 37oC overnight then the wells were washed with a washing buffer. Two hundred micro liters of a blocking solution were added into well and incubated for 1 hour. After discarding the fluid from the well, well was extensively washed with PBST to remove unbound phages. The fluid was then added into a well containing 200 µl of HB2151 E.coli which had been grown to log-phase and the well was incubated at 37oC for 5 minutes. An aliquot of 66 µl was used to spread onto each 2x YT agar plate containing 100 µg/ml of ampicillin and 2% glucose (2x YT-AG) and the phages were incubated at 37oC overnight.

3. Determination of E.coli colonies with husvFv-phagemids

For determining the transformed E.coli that carried the husvFv-phagemid, a small portion of the bacterial colonies on the 2x YT-AG plate were randomly picked and a replica plate was made. Bacteria of the same colony remaining on the loop were inoculated into 100 µl of distilled water and used directly as DNA template for checking the presence of the huscFv by PCR. The PCR was carried out using a specific pair of primers. After amplification, the PCR products were analyzed for the presence of huscFv by a 1% agarose gel electrophoresis and ethidium bromide staining. The PCR products were also subjected to MvaI restriction endonuclease digestion for determining the restriction fragment length polymorphism (RFLP) of the huscFv sequences derived from individual phage clones.

4. Verification of the HuScFv binding activity to recombinant Nef protein

The HB2151 E.coli colonies that gave positive huscFv amplicons of the expected size (~1,000 bp) were picked from the replica 2x YT-A broth containing 1 mM IPTG. For verification of the ability to express HuScFV, the E.coli cells were suspended in PBS and subjected to sonication by using the ultrasonic homogenizer LABSONIC P at 40% amplitude for 0.5 cycles in an ice bath. The bacterial homogenate was centrifuged at 12,000 x g at 4 oC for 10 minutes; the supernatant (bacterial lysate) was subjected to an indirect ELISA (HuScFv-ELISA) for detecting the binding specificities of the HuScFv to the respective recombinant Nef protein.

Results

The recombinant Nef protein was used as antigen in phage bio-panning to select phage clones that displayed HuScFv. From 60 randomly selected transformed E.coli clones (Fig.1) derived from phage bio-panning with recombinant Nef. Twelve clones huscFv sequences. (Fig.2)

Fig.3 shows MvaI-cut-DNA banding patterns of the huscFv sequences of the 1-12 transformed HB2151 E.coli clones that expressed HuScFv bound to the recombinant Nef protein. Twelve different RFLP patterns were found among the huscFv sequences of the 12 E.coli clones that produces HuScFv to the recombinant PB1 (lanes 1-12).

HuScFv prepared from huscFv positive E.coli clones were tested by indirect ELISA for their binding activity to the homologous proteins. Fig.4 shows the indirect ELISA results of HuScFv from transformed HB2151 E.coli that gave positive binding to the homologous recombinant Nef protein. HuScFv prepared from 4 of the 12 HuScFv expressing clones, i.e., clones 3, 7, 9, 10, could bind to the recombinant Nef with significant ELISA OD (two times higher than OD of BSA which was used as the control).

Fig1. Transformed *E.coli* clones

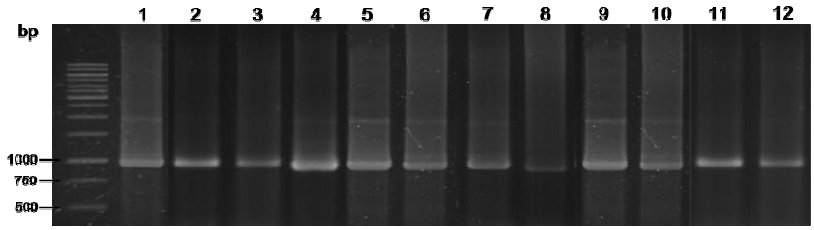

Fig2. Results of agarose gel electrophoresis of the PCR amplicons for detecting the presence of *huscFv* sequences in transformed HB2151 *E.coli* clones harboring *huscFv*-pCANTEB5E phagemids derived from bio-panning with the recombinant Nef. Lanes M, 1 kb DNA ladder.

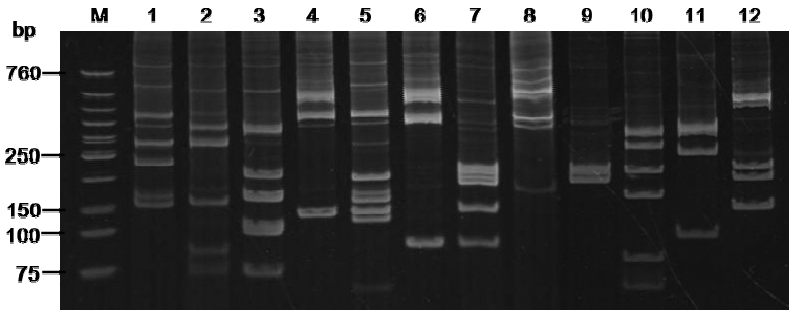

Fig3. DNA banding patterns for determining RFLP of *Mva*I-cut *huscFv* amplified from recombinant pCANTA-BE5 phagemids transformed HB2151 *E.coli* clones. Lanes 1-12, DNA banding patterns clones 1-12, respectively. Lane M, Low molecular size DNA ladder.

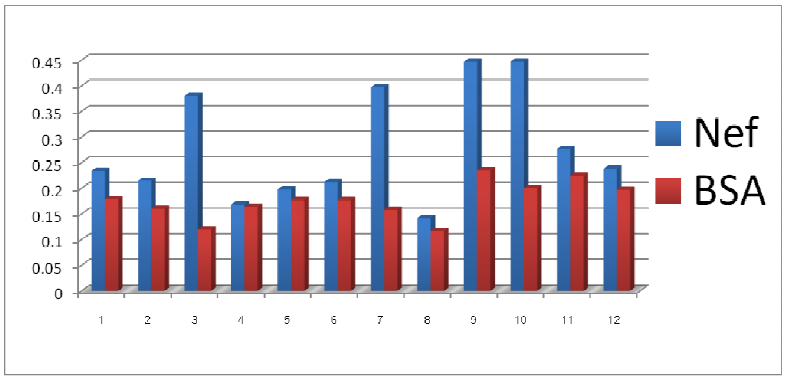

Fig4. Results of the HuScFv-ELISA for the detection of the binding of HuScFv expressed from the transformed
HB2151 *E.coli* clones to the recombinant Nef.

Conclusion and Discussion

According to the result from all experiments, we can conclude that there were 12 different patterns of ScFv molecule specific for Nef protein of HIV-*1.* And at least *4* clones were exactly specific to Nef protein.

For future work, these ScFv will be tested for Nef protein inhibiting efficiency for developing immunotherapy. Then there should be an availability of *huScFv* that binds specifically to Nef protein.By interfering with Nef functions, the immune effector functions response to HIV should be restore, which would help the body to fight against the HIV infection

Acknowledgement

The work was financially supported by Faculty of Medicine, Siriraj Hospital, Mahidol University, Bangkok, Thailand under the grant awarded to Dr. Nitat Sookrung.

References

1. Umaporn T. et al., Human Moclonal Single Chain Antibodies(HuScFv) that Bind to the Polymerase Proteins of Influenza
A virus, Asian Pac J.Allerg Immunol. *(*2006) 26: 23-35

Comparative studies of leaf anatomy of *Bougainvillea* sp.

Chanatip Chailek and Somruthai Homchuen
Mahidol Wittayanusorn School, Salaya, Buddhamonthon, Nakorn Pathom, Thailand

Abstract

Bougainvillea is a common plant decorating garden in Thailand because of Bract which is colorful and differ from foliage leaf. Comparative studies of leaf anatomy of *Bougainvillea* sp. at Mahidol Wittayanusorn School. To delineate differences in their epidermal cell, stomatal index, stomatal size and leaf anatomy to recognize their physiological behavior, was investigated with light microscope using epidermal peel and transverse sections. The epidermal cells of bract were amorphous with rough surfaces; conversely, epidermal cells of leaf were polygonal. The stomatal complex in both organs was anomocytic. The stomatal index was greater on the abaxial surfaces of the leaf than their corresponding adaxial surfaces and bract. Furthermore, leaf anatomy showed the phloem of Bract is located on the opposite side of xylem that differs from Nyctaginacea character reported by Evert, Ray F. (2006). This study clearly illustrates morphological disparities in the epidermal features of leaf and bract, helping to explain their physiological divergence.

Introduction

Bougainvillea (*Bougainvillea* sp.) was classified in family of Nyctaginacea. Its *attractive leaf* or *bract*, which is a modified leaf associated with flower; each cluster of three flowers is surrounded by three bracts, are brightly colored and serve the function of attracting pollinators instead of petal (Chittraphorn, 2005; Linda R. Berg, 2006), therefore, they are important for this plant. (There is no the report on anatomy and epidermis morphology of bract) The investigation provides study on comparison of the leaf epidermal features and leaf anatomy of foliage leaf and bract of this plant.

Objective

This study aims to delineate differences in epidermal features and anatomy of foliage leaf and bract, such information would be useful in explaining their functions.

Materials and Methods

Plant material

Bougainvillea (*Bougainvillea* sp.) plants were grown for being ornamented the garden at Mahidol Wittayanusorn School, Nakorn Pathom, Thailand. Leaf materials were randomly select from the top of branch.

Study on Leaf epidermal features

Peel leaf skin then observe epidermis using light microscope, included epidermal cell, type of stomatal complex, stomatal size and stomatal index according to Salisbury's (1927) formula: SI = s/(e+s) x 100 where s for the number of stomata per unit area and e is the number of epidermal cells in the same area

Study on Leaf anatomy

Free hand leaf cross section, then observe using light microscope.

Results

1. Leaf epidermal features

(A) (B) (C)

Figure 1 Epidermal features

(A) Adaxial surface of foliage leaf
(B) Abaxial surfaces of foliage leaf
(C) Bract

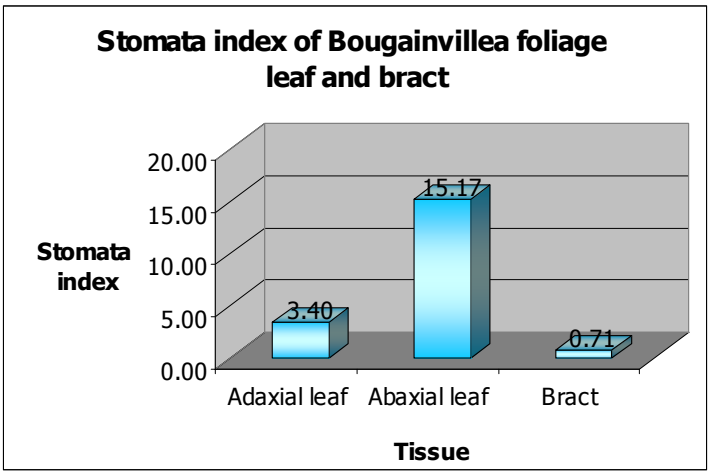

Figure 2 Stomata index of Bougainvillea foliage leaf and bract

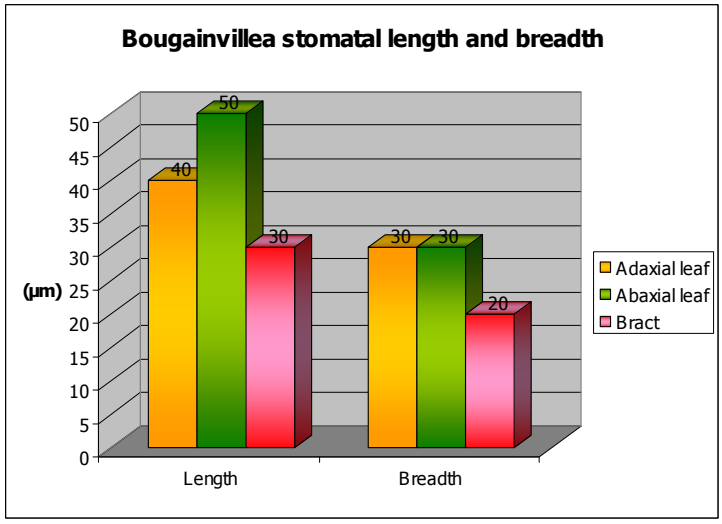

Figure 3 Bougainvillea stomatal length and breadth

Discussion & Conclusion

The epidermal cells of bract were amorphous with rough surfaces. Similar epidermal cells were reported by Michelle M. M. (1988) in potato (*Solanum tuberosum*) leaf, on the other hand, epidermal cells of leaf were polygonal. A type of stomata on both leaf and bract were anomocytic. The stomatal index (SI) of abaxial surface of leaf was greater than adaxial surface and bract significantly. The bracts, grows inside the canopy, under a shaded habitat. Thus, the shaded habitat of the bract may explain their lower SI compared with that of the leaf (Bondada, 2000). Stomatal length was varied on gas exchange and stomata transpiration. (LI Qiang et al., 2007)

The anatomy of leaf was different from bract. Phloem of Bract is located on the opposite side called external and internal phloem, not according to Evert, Ray F.(2006) which explained Nyctaginacea producing phloem outward and xylem inward. Bract didn't have palisade mesophyll.

The result from the study distinctively showed the difference in epidermal features and anatomy of the foliage leaf and bract. These epidermal variations provide a strong morphological basis to elucidate the disparities in their physiological behavior (Bondada, 2000).

Reference

Bondada, Bhaskaer R. and Oosterhuis. (2000). **Comparative Epidermal Ultrastructure of Cotton (Gossypium hirsutum L.) Leaf, Bract and Capsule Wall**. Annals of Botany 86: 1143-1152.

Evert, Ray Franklin. (2006). **Esau's Plant Anatomy: meristems, cells, and tissue for the plant body: their structure, function and development**. 3rd ed. New Jersy, USA: John Willey & Sons, Inc.

Detection and typing of Dengue viruses from *Aedes* sp. by using One-step Reverse Transcriptase-Polymerase Chain Reaction (One-step RT-PCR)

Pichanon Mingchay[1], Supanan Sae-Lim[1],
Padet Siriyasatien[2], Vorraphun Yingsiwaphat[3]
[1]Mahidol Wittayanusorn School, [2]Department of Parasitology, Faculty of Medicine, Chulalongkorn University,
[3]Biomedical Science Program, Graduate School, Chulalongkorn University

ABSTRACT

To study dengue virus infection rate in the mosquito vectors (*Aedes aegypti* and *Aedes albopictus*). The mosquitoes were collected from Nakhon Pathom and Samutsakhon province during winter season. The dengue viruses were detected using One-step Reverse Transcriptase-Polymerase Chain Reaction (One-step RT-PCR). The result showed that the virus infection rate in mosquito collected from Nakhon Pathom and Samutsakhon province was 79% and 11% respectively. This project provided the support information to find the best- operation for dengue outbreak control.

INTRODUCTION

Dengue hemorrhagic fever (DHF) remains a major health problem in Thailand and Southeast Asia. The infection is caused by single-stranded RNA virus (Family *Flaviviridae* , Genus *Flavivirus*) which vary to 4 serotypes (DEN-1,DEN-2,DEN-3,DEN-4). Dengue virus is transmitted to human via the bite of mosquitoes. *Aedes aegypti* and *Aedes albopictus* are major vectors of dengue transmission in Thailand. The patient who is infected by dengue virus may develop fever, pinpoint spots of blood on the skin, shock and death.

In Thailand, the dengue control relies solely on destroyer for *Aedes* larval habitat and mosquito control. Although the control method has been regular operated for many years the report of dengue outbreak has never decreased. Apart from mosquito density data, the virus infection rate in mosquito should be combined with other indicators for predicting dengue outbreak. In this study, we demonstrated the dengue virus infection from field-caught mosquitoes using One-step Reverse Transcriptase-Polymerase Chain Reaction (One-step RT-PCR) and analyzed the infection rate in Nakhon Pathom and Samutsakhon province during winter season.

PURPOSE

To study the dengue infection rate and identify the dengue serotype from field-caught mosquitoes in Nakhon Pathom and Samutsakhon province.

MATERIALS AND METHODS

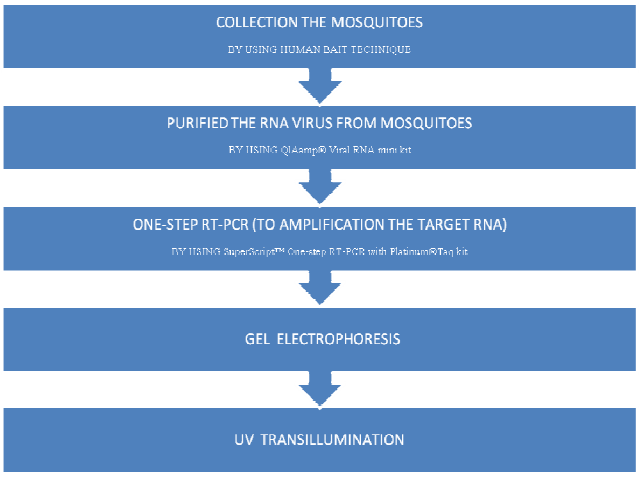

RESULT

			Nakhon Pathom province (%)	Samutsakhon province (%)
Mosquitoes negative for virus			21	87
Mosquitoes positive for virus	single serotype	DEN-1	26	8
		DEN-2	0	3
		DEN-3	32	0
		DEN-4	11	0
	multiple serotypes	DEN-1 & DEN-2	0	0
		DEN-1 & DEN-3	5	0
		DEN-1 & DEN-4	0	0
		DEN-2 & DEN-3	0	0
		DEN-2 & DEN-4	0	0
		DEN-3 & DEN-4	5	0

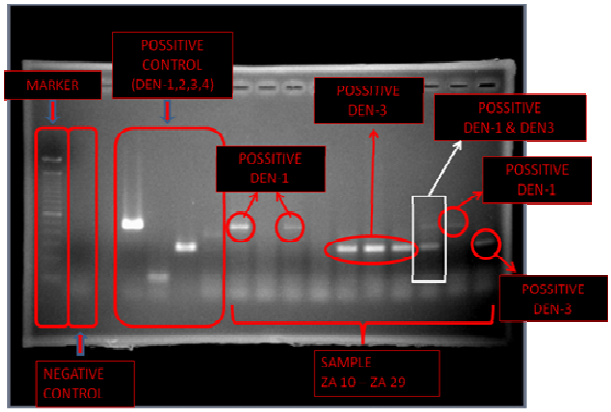

DISCUSSION

We report the infection of dengue virus from field caught mosquitoes. This result demonstrated that dengue virus could be found in single serotype or multiple serotypes. The multiple serotypes are caused by double infection of dengue virus in mosquito, whith different serotype. Advantages of the One-step Reverse Transcriptase-Polymerase Chain Reaction (One-step RT-PCR) used in this study including more simple, cheaper and easier than the methods reported previously. Moreover, One-step RT-PCR is a short-time method, it can detect dengue virus within 6 hours. From our report, Nakhon Pathom should be considered for dengue problem and use operation to control before the dengue outbreak.

CONCLUSION

The infection rate for dengue virus in mosquitoes, by using One-step Reverse Transcriptase-Polymerase Chain Reaction (One-step RT-PCR) technique, in Nakhon Pathom province was 79% and in Samutsakhon province was 11%. Among the 4 serotypes, the DEN-3 was the highest infection rate in mosquitoes collected from Nakhon Pathom with 32% of infection. The dengue infection rate in mosquito should be considered as an index for predicting the dengue outbreak, therefore dengue control strategies will be applied more effectively.

ACKNOWLEDGEMENTS

The author is grateful thanks to Department of Parasitology, Faculty of Medicine, Chulalongkorn University and Mahidol Wittayanusorn School, for all of supports for this project. And we thank all of staffs in Chulalongkorn University.

REFERENCES

Lanciotti RS, Calisher CH, Gubler DJ, Chang GJ, Vorndam AV.Rapid detection and typing of dengue viruses from clinical samples by using greverse transcriptase-polymerase chain reaction. J Clin Microbiol. 1992 Mar;30(3):545-51.

Thavara U, Siriyasatien P, Tawatsin A, Asavadachanukorn P, Anantapreecha S,Wongwanich R, Mulla MS.Double infection of heteroserotypes of dengue viruses in field populations of *Aedes aegypti* and *Aedes*

Bio Stealth – Making Perfect Transparency

Shun Yoshida
Ritsumeikan High School

Introduction

What would the world be like if humans could be made invisible? People young and old have considered this question. In some comics or movies, e.g. The Predator, there are characters or items that can not be seen. Of course, these examples are fictional, but maybe sometime in the future this could happen in reality.

Background Information

There are already some examples of living things that can alter their appearance. Some Octopuses can change their color and shape to blend in with the background. This is a useful form of camouflage as it means they can hide from predators and prey. Chameleons and Plaice can also adapt their skin color to make them appear almost invisible.

Students at Tokyo University are currently researching a concept known as 'active camouflage'. They have made a camouflaged object appear almost invisible. Active camouflage can be used in many situations as the appearance of the camouflaged object changes to match its surroundings. The United States Army is currently using Massachusetts Institute of Technology (MIT) to investigate how to make things transparent.

A Retro-Reflector is a material that could be used for making things transparent. It is made from glass beads and used in road signs. Retro-Reflectors are useful because they reflect light back to the light source. The angle of incidence is not the same as the angle of reflection, unlike conventional mirrors.

Bio Stealth Project

Considering the previous research into this topic I named this project 'Bio Stealth'. The aim of these tests was to find out if both still and moving images could be seen clearly through a retro reflector.

Experiment one (a still image)

Method

1. Using a USB camera a photo of a background image was taken.
2. The photo was projected onto a wall.
3. A projector provided the light source and the light was reflected onto the retro reflector using glass.

The image was viewed from in front of the retro reflector.

Here is a diagram of the apparatus:

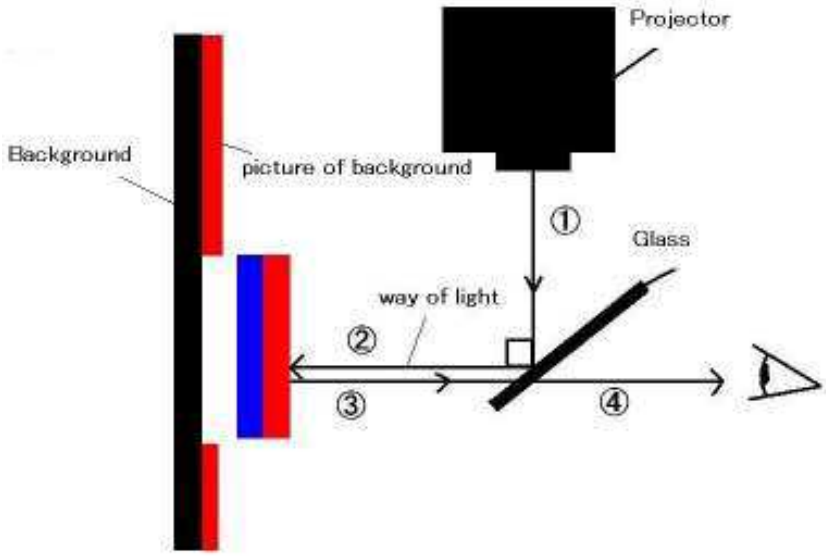

Result

The photo could be seen clearly. This was because the light was reflected back towards the eye. It was almost perfectly transparent.

Experiment two (a moving image)

Method

1. A USB camera was used to make a live video recording.
2. These images were projected in front of the retro reflector. All other things were the same as in experiment one.

Here is a diagram of the apparatus:

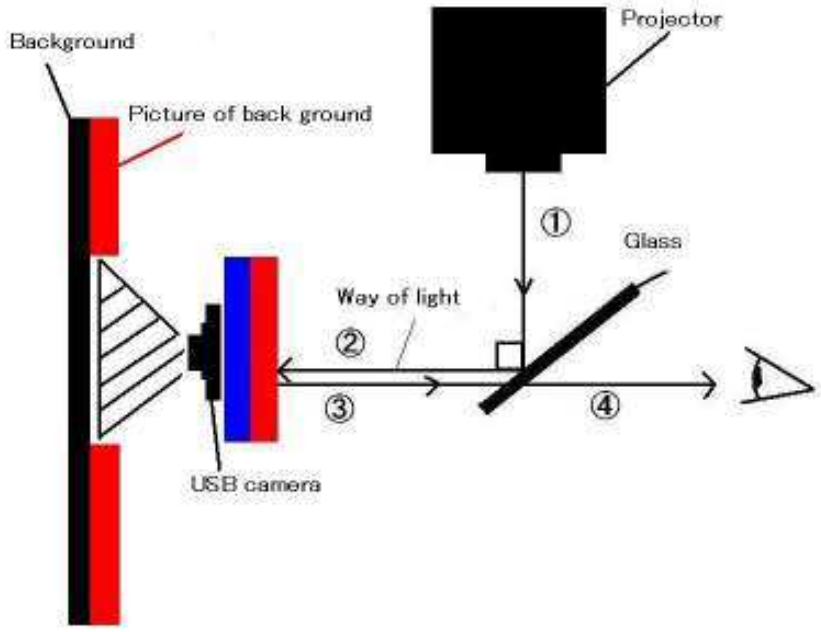

Result
The image could be viewed but the transparency wasn't as good as with the still image.

Limitations of Bio Stealth project
It was difficult to make improvements to the performance of Bio Stealth. I could not find a way to perfectly match the picture with the background despite making many fine adjustments. Similarly I found that the projector was not a good light source. It was too big and projectors are not practical items for carrying out experiments outside of a laboratory. An Organic Light Emitting Diode TV would be a better light source because they can project a live video by themselves. They are also thinner and lighter than projectors.

Future Plans
This project is only one month old. Experiments need to be carried out over a longer period of time before more accurate findings can be made. Arguably a combination of an animal camouflage system, e.g. the chameleon, and advanced computer techniques could improve the performance of Bio Stealth.

List of References

http://ja.wikipedia.org/wiki/%E5%85%89%E5%AD%A6%E8%BF%B7%E5%BD%A9

http://upload.wikimedia.org/wikipedia/commons/thumb/a...

http://www.flickr.com/photos/maynard/146081479/

http://response.jp/issue/200http://glassmoon.seesaa.net/...

http://www.bidders.co.jp/item/66069206

http://glassmoon.seesaa.net/article/1346160.html

http://aesthetica.arrow.jp/blog/

Biodiesel Renewable but Toxic.

Ross Tieman[1] and Ashleigh Fields[1] ,Dr. Richard Bentham[2]
1. **Australian Science and Mathematics School**
2. Department of Environmental Health Flinders University, Adelaide

ABSTRACT
This investigation was designed to find the potential effects that biodiesel may have on plant growth and germination. Soil was contaminated with various amounts of biodiesel, lupins (*Lupinus angustifolia*) were planted and growth and germination measured. It was found that contaminations of 2:100 ml:g or greater inhibited growth and germination significantly

INTRODUCTION
Biodiesel is a fuel derived from natural sources such as vegetable oils and animal fats. We know biodiesel is a more cost efficient fuel and also easily accessible, but do we actually know if biodiesel is environmentally friendly? What we do know is that biodiesel is biodegradable, a renewable fuel and reduces air pollutants.

METHOD
The biodiesel used throughout this investigation is referred to as B100 (pure biodiesel). The experiment was conducted over an eight week period. Three replicates of potting mix were contaminated with biodiesel at levels of 1:100, 2:100 or 3:100ml:g, with a control batch consisting of uncontaminated soil. For each batch there were three pots containing 15 lupin seeds in each pot. The seeds were given four weeks to germinate prior to the first set of measurements. Measurements consisted of sacrificing one pot of each treatments. Root length, shoot length and biomass were then measured for each pot. The same measurements were taken at 6 weeks and 8 weeks after germination.

RESULTS

The control and 1:100mg:g biodiesel showed normal growth. The 2;100 and 3:100mg:g biodiesel showed greatly reduced growth and germination. Both the control and biodiesel one had 'nodules' present on roots which are a sign of healthy plant growth, these nodules were not present on biodiesel treatments two and three.

Measurement 3 (Wk 8)	Root	Shoot	Biomass
Control	231.36	245.54	0.5471
Biodiesel 1	107	201.86	0.2711
Biodiesel 2	91.25	122.5	0.1598
Biodiesel 3	65.57	163.28	0.1983

Measurement 2 (Wk 6)	Root	Shoot	Biomass
Control	117.44	201.55	0.2038
Biodiesel 1	102.12	175.35	0.1805
Biodiesel 2	96.75	184.82	0.1954
Biodiesel 3	64	152.75	0.1527

Measurement 1 (Wk 4)	Root	Shoot	Biomass
Control	81.88	117.13	0.0971
Biodiesel 1	65.5	127	0.1028
Biodiesel 2	76.88	138.67	0.1208
Biodiesel 3	33.75	60.13	0.0745

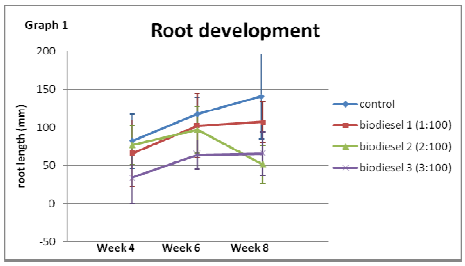

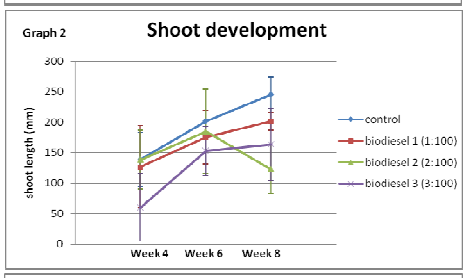

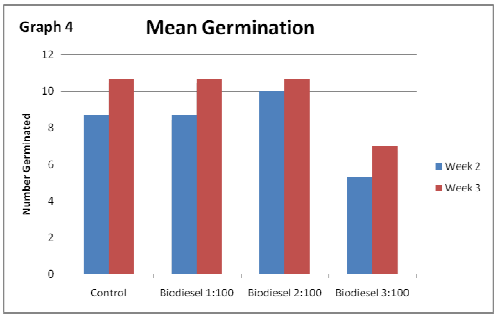

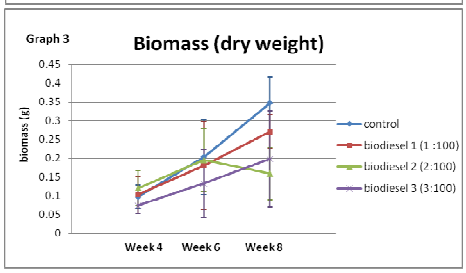

CONCLUSION

Biodiesel contaminated soil with concentrations of 2% biodiesel or greater showed discernibly inhibited growth over an 8 week period. Biodiesel contaminated soil consisting of 3% biodiesel effected seed germination both in time taken to germinate and total amount of germinations. The overall plant health was effected by the biodiesel, with the lupins in soil with concentrations greater than 1% biodiesel having no nodules present on the roots which is a sign of normal health.

ACKNOWLEDGEMENTS

A special thanks to all of the Environmental Health Department of Flinders University, Adelaide.

References

- *BAA*, http://www.biodiesel.org.au/, [Online accessed 22 Oct 2007]Page last modified: Unknown.
- *Fifteen facts about biodiesel*, http://www.biodiesel.org.au/biodieselfacts.htm, [Online accessed 22 Oct 2007]Page last modified: Unknown.

Design and Development of a Novel True Power Measurement Device

Luke Victor Australian Science and Mathematics School,
Dr Wen Soong Electronic Engineering Department, Adelaide University, SA.

Introduction

Global Warming— We all know that global warming is a current world issue. One of the major contributors to the worlds greenhouse gas emissions comes from power generation and the burning of fossil fuels. In order to minimize the effect of global warming, greenhouse gasses will need to be reduced. One way of reducing greenhouse gas output is to minimize the wastage of big producers, such as energy.

A cheap power meter to check which appliances are using the most energy would be extremely useful in examining household energy consumption and wastage. This project aims to design and build a small, cheap and effective power meter which measures 'true' power.

What is True Power?

True power is a term which refers to the actual power used by an appliance, not in theory, but in practice. There is a formula to define the relation ship between current, voltage, phase shift and the true power.:

$$P=V.I.(\cos\emptyset)$$

where P is the true power (in watts), V is the voltage (in volts), I is the current (in amperes) and Ø is the angle of the phase shift (in degrees). This relationship is true for all sine-wave patterns, as shown below in **Diagram 1.**

Diagram 1: A simple sine wave.

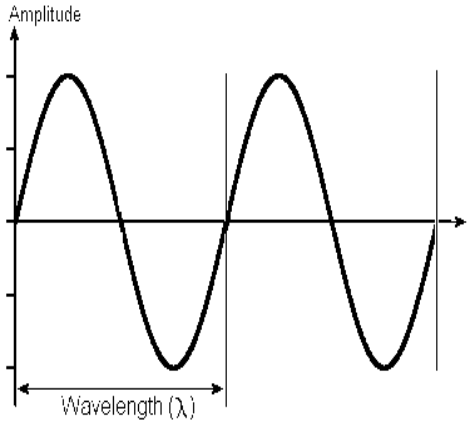

Because this is a difficult calculation, the time taken for an IC chip to come up with a final answer would take too long, and the sample rate of the device (number of samples per second) would not be high enough to accurately represent the changing value of power over a period of time.

Since this project is meant to result in a cheap and effective meter, a more effective method must be used, such as utilizing hardware to do most of the hard work hence saving a lot of time on the sampling rate, as well as improving the overall accuracy. The method used made use of a 'flipping' theory which he had discovered some time ago, which 'flips' the current when the voltage is negative.

What is 'Flipping'?

There are two interacting sine waves (voltage and current) when measuring power, as shown in **Diagram 2**.

Diagram 2: Comparison of voltage and current sine waves.

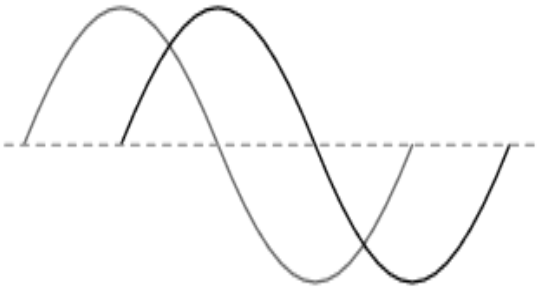

In essence, using 'flipping', removes the need for calculating the phase shift at all, by making the current and voltage into a representation of power. (a positive current and positive voltage = positive power, positive current and negative voltage =negative power, negative current and negative voltage = positive power).

Diagram 3: Power wave produced by 'flipping' the waves in Diagram 2.

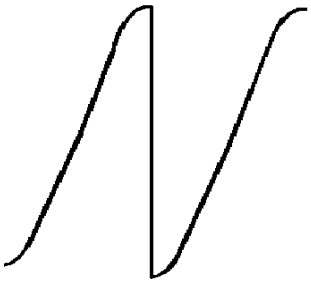

The resultant power wave (a graphical representation of the power used over time) of the sine waves above is shown in **Diagram 3**.

The power wave produced by 'flipping' spends equal amounts of time above and below the '0' line, which averages out to make the overall power reading 0 watts. This is the sort of wave which confuses other methods of power measurement.

What Did We Do?

The first stage was to design a circuit which can successfully invert the current based on whether or not the voltage signal is negative. The circuit is designed to use the voltage signal as a basis on whether or not to invert the current, so that when the voltage is negative, the current is inverted.

After designing, building and testing this circuit, the focus turned to designing a circuit to fit into a box, and connect to an LCD display. The final prototype was fitted into a box, with an LCD display and three buttons, which are in place to allow for adjusting cost and voltage at a later date. On the LCD display is a readout of the current power usage (in kilowatts), the total energy usage (in kilowatt hours) the total running time since last restart (in hours) and the total cost (in dollars and cents).

Future Directions?

It is planned to continue this development until such time as the device has reached a stage at which it can be commercialized in order to help reduce wastage of electricity in households, and hence reduce the impact of greenhouse gasses and the global warming effect.

Acknowledgments.

Thanks to Dr Wen Soong, Staff of the Dept. Electronic Engineering, Adelaide University and elabtronics.

The Effect of Grey Water on *Cherax destructor*

James Galbraith, Laura Stradling - Australian Science and Mathematics School
Dr Kirstin Ross - Dept. Environmental Health, Flinders University.

Background

Water is our most precious resource. As reservoirs and rivers are running low in water (The Economist, 2007) we are looking for better ways to use current water resources (UNESCO, 2006). One possible solution to maximise water resources in aquaculture is by reusing grey water (water discharged from household appliances like dishwashers and washing machines and from sinks, showers and bathtubs). (SA Water, 2004) .

However, there are several limits to grey water use including that grey water might be contaminated. These contaminants might include harmful micro-organisms, traces of faeces, urine, blood, dirt, lint, food scraps, hair, body cells and fats . Other contaminants include chemicals from soaps, shampoos, dyes, mouthwash, toothpaste, detergents, bleaches or disinfectants.

The Australian Yabby, *Cherax destructor* is a semi aquatic fresh water crustacean, found throughout the eastern parts of Australia. Yabbies live in diverse environments, with variations in salinity, dissolved oxygen content, flora and fauna. Yabbies can live in water temperatures between 0 and 35°C, with the ideal range being between 20 and 25°.

Purpose

The purpose of this experiment was to investigate the level of tolerance of the Australian Yabby, *Cherax destructor*, to grey water, with the ultimate goal to assess its suigalb0010tability as an aquaculture species living in grey water.

Method

In the first part of the investigation 10 yabbies were each exposed to aged grey water, new grey water or control of de-chlorinated tap water. In the second part of the experiment, 10 yabbies were exposed to new grey water concentrations of 1×, 10×, 100×; or a control of de-chlorinated tap water.

The grey water used was artificial due to health and safety issues.

Analysis

As shown in Graph 1, there was 100% survival in the control and aged grey water after the full 96 hours. In the 0.25× new grey water 10% of the yabbies died after spending 48 hours , with the remaining 90% surviving the full 96 hours. In Graph 2 there was an overall pattern of decreasing yabby survival with increasing grey water concentration (Graph 2). The control yabbies had 90% survival after 24hrs, with no further losses. The 1×grey water had 10% of the yabbies die in the first 24 hours, with the remaining 90% surviving the term of the experiment. The 10× grey water resulted in 20% mortality after 24 hours with the remaining yabbies surviving the full 96 hours. In the 100× concentration 80% of the yabbies died in the first 24 hours, with the remaining yabbies dying after 48 hours.

Graph 1 - Effect of new and aged 0.25× Concentration

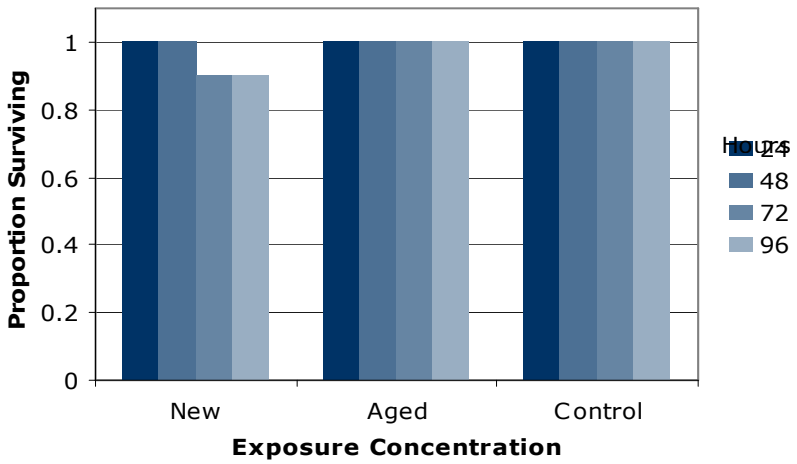

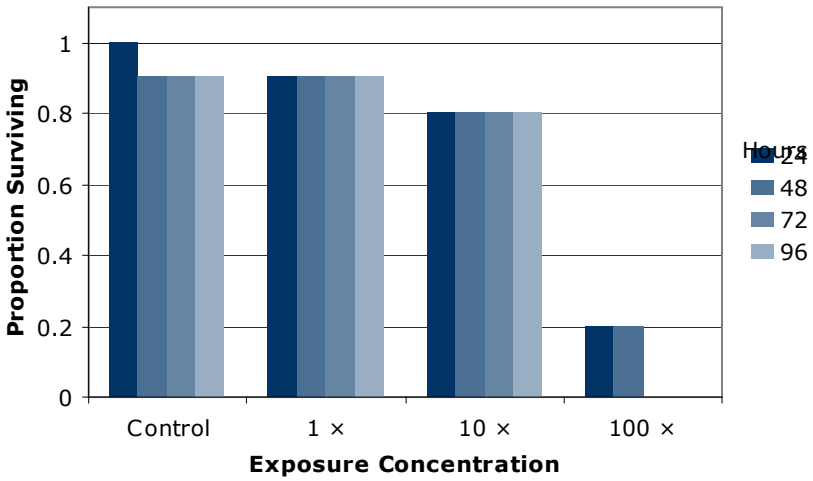

Conclusion

Yabbies commonly live in a hard water environment like dams and creeks (NSW Department of Primary Industries,2005), where mineral content is high . Because of this it is likely the water that they naturally live in is harder (has a higher mineral content) than the artificial grey water used in the experiment.

The 0.25× and 1× concentrations may have had minimal effect on the yabbies because the water they normally live in is more polluted than the water used in this experiment. On the other hand, it is highly likely that the yabbies in the 100× concentration died due to its toxicity.

The yabbies may have died as a result of stress. Because the water was changed frequently, the yabbies were being handled often and their environment was changing. These yabbies in the grey water had the largest change in habitat (different colour content and coloured water). Alternatively the yabbies may have died as a combination of both factors.

From this experiment it is possible to conclude that yabbies are largely tolerant to new and aged grey water in normal and slightly higher concentrations. This makes an ideal species for use in aquaculture.

Acknowledgements

Thanks to Dr Andrew Stone and Cat Stone for their patience, guidance and help; to Dr Richard Bentham for his witty suggestions and humour and to all those in Dept of Environmental Health who put up with us.

References

Bibliography

The Economist, *Australia's water shortage*,http://www.economist.com/world/displaystory.cfm?story_id=9071007, published April 26 2007.

United Nations Educational, Scientific and Cultural Organization, *2nd UN World Water Development Report*, http://www.unesco.org/water/wwap/wwdr2/table_contents.shtml, published March 2007

SA Water, *Greywater and Recycled Water* , http://www.sawater.com.au/SAWater/YourHome/SaveWaterInYourGarden/Greywater+and+Recycled+Water.htm, last edited June 9 2007.

NSW Department of Primary Industries, *Yabby - aquaculture prospects*, http://www.dpi.nsw.gov.au/fisheries/aquaculture/publications/species-freshwater/freshwater-yabby, last edited October 2007.

Photos

Aquaculture Council of Western Australia, http://www.aquaculturecouncilwa.com/yabby.jpg.

NSW Water Bug Survey, http://www.bugsurvey.nsw.gov.au/html/popups/images/lge_fr-ya_col.jpg.

The effects of Endophytic Actinobacteria isolated from *Lucerne* against fungal root diseases.

By Courtney Mason, Australian Science and Maths School

Abstract

This project is aimed at using Endophytic Actinobacteria as a possible biological control method for controlling fungal disease within wheat and pasture species by testing their antibiotic production potential.
Samples of *Lucerne* (a commonly used pasture species in South Australia) were obtained and used to isolate Actinobacteria colonies. These colonies were then isolated further to ensure purification.
The pure isolates were streaked upon agar plates with one four different types of fungi. Three replicates of each isolate plate were made with each fungus, as well as replicate sets of control plates, for comparison. The plates were incubated which allowed the Actinobacteria and the fungus to grow.
After the incubation period, the plates were viewed to see the effects that had taken place. The growth of the fungus in the presence and absence of the Actinobacteria were compared.
The plates showed that most of the Actinobacteria isolates produced enough antibiotics to limit fungal development, this created a zone of inhibition between the Actinobacteria and the fungus.
The results have shown that Actinobacteria are a possible biological control method of fungal diseases due to their antibiotic potential.

Introduction

Wheat and pasture grasses within Australia are affected by numerous fungal root diseases. This is due to restrictions and lack of suitable chemical control methods. These diseases negatively affects the overall production rate, yield and income achieved for many farmers due to a loss of crop. This research aims to find a biological control for these fungal diseases using Endophytic Actinobacteria.

Actinobacteria are a group of gram-positive, filamentous bacteria that sporulate. Actinobacteria mainly inhabit soil Environments, however Endophytic Actinobacteria live within plant roots and tissue. Actinobacteria produce secondary metabolites, such as antibiotics and plant growth regulators.

Method

Part 1: Isolation

1. Obtain *Lucerne* plant samples.
2. Wash *Lucerne* thoroughly with water to remove soil and other organic matter.
3. Surface sterilise roots using ethanol, sodium hypochlorite and RO water.
4. Cut roots into 1cm pieces and place 20-30 pieces upon Starch Casein(SCA) and Humic Acid with Vitamin B(HVB) plates.
5. Incubate plates at 27^0 and 37^0 C.

Possible Actinobacteria Colonies.

Surface sterilised *Lucerne* roots upon HVB

Part 2 : Purification

6. Isolate Actinobacteria colonies using a loop and streak onto a Potato Dextrose(PDA) plate.
7. Incubate all plates again.

Isolation plates

Non contaminated plate

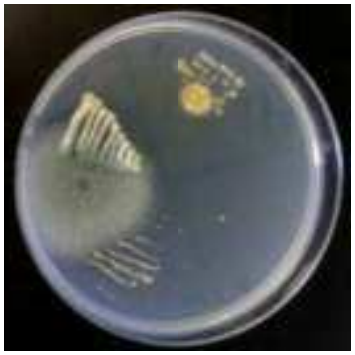

Plate with fungal contamination

Pure Actinobacteria isolation plate.

Each pure isolate is given an isolate number. Nine isolates were used: C1, C5, C7, C11, C12, C17, C29, C50 and C51.

Part 3 : Testing for anti-fungal activity

8. Streak one third of a Cornmeal agar(CMA) plate with pure isolates using a loop. Make three replicate plates of each isolate for each of the fungus species.
9. Incubate at 27^0 and allow to grow for 10 days.

After incubation period place a cube of fungi on each plate, using different types of fungi. Ensure control plates without
Actinobacteria are made for each fungus
species.

11. Reincubate and allow to grow for four days.
12. Check plates and measure the growth of the fungi towards the Actinobacteria and upon the control plates. Record results.
13. Reincubate for another 3 days and then
remeasure and record results.

Day 4
Control plate,
Rhiz Rep 3

Day 7
Control plate,

Day 4
C51 Rhiz Rep 3

Day 7
C51 Rhiz Rep 3

Fungi used

Pythium irregulare (**Py**), *Fusarium oxysporum (***Fus ox***)*, *Rhizoctonia solani AG8* (**Rhiz**) and *Gaemannomyces graminis var trici* (**Ggt 8**)were used because each fungi will be differently affected by the Actinobacteria.

Important factors

There were a few factors which contributed to varying the outcome of the results.

- The isolates were incubated at 27^0 and 37^0C whilst being purified, whereas the experimental plates were only incubated at 27^0. This is because within a normal soil environment the fungi would not be exposed to temperatures higher than 27^0 .
- Py could only be measured once because the control plate was completely covered in growth on Day 4 (therefore the Day 7 results are lower than they should be because there was no recent control ratio to be used).
- The Ggt8 control plates fungal growth was limited, yet it grew more profoundly on the isolate plates, this affected the results by lowering the average.

Determining Results

To determine the amount of antifungal activity of the Actinobacteria the radius of the control plate and the radius of the growth on the isolate plate towards the Actinobacteria were taken and then applied to this formula:

$$\frac{\text{Control radius}}{\text{Fungus plate radius towards Actinobacteria}}$$

An average ratio was then determined from each of the replicate isolate plates and controls.

Day 7, C7 Ggt8 Rep2
The ratio
towards the
Actinobacteria that is being measured.

Zone of
Inhibition.

Results

Of the isolates obtained there were representatives of several genera of Actinobacteria, including: *Streptomyces*, *Microbispora* and *Micromonospora*.

To determine the isolates antifungal potential, their average ratio was compared with a rating system. This helps to verify the most productive isolates.

Antifungal Activity	Ratio
Very Strong	≥ 5
Strong	≥ 3.5 - <5
Moderate	≥ 2 - <3.5
Weak	≥1- <2

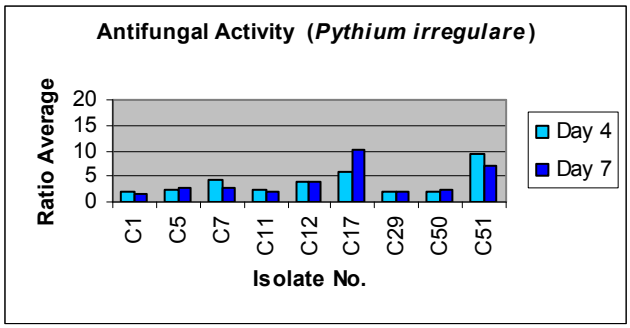

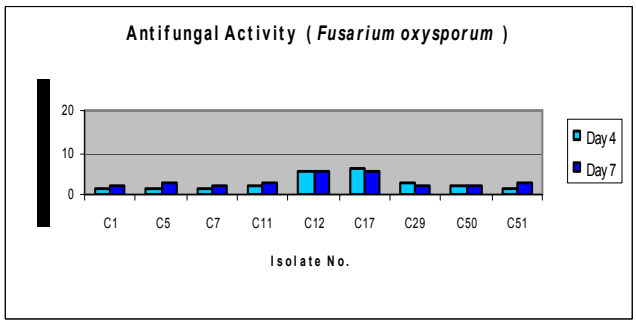

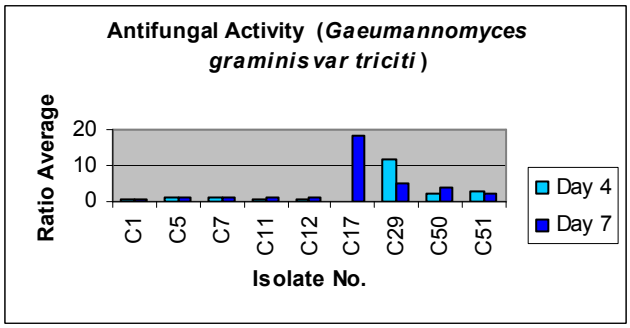

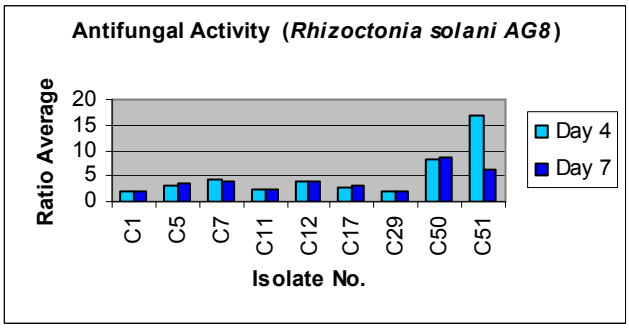

The most effective isolates for fungal control
appear to be C17 and C51 because each have
produced enough antibiotic to limit the fungal growth therefore raising their ratio to over 5 numerous times.

The graphs also show that antibiotic production continued to Day 7. Some plates also did not
exhibit a zone of inhibition because the isolate was not effective in controlling the fungi.

This experiment has shown that Endophytic
Actinobacteria are a possible biological control of fungal root disease. Future testing will confirm their effectiveness.

Future Testing

- The isolates obtained will be used to
inoculate Lucerne seeds which will be placed within a soil environment containing one of the fungal diseases, then allowed to grow within a controlled greenhouse environment.
Germination and growth of the plant will be measured to determine if there is protection from the Actinobacteria against the disease.
- The overall most promising isolates will be used within field trials.

Acknowledgements

Special thanks to Flinders University
Department of Medical Biotechnology, Phil
Michelsen and Professor Christopher Franco for all their guidance on this project.

AUSTRALIAN SCIENCE & MATHEMATICS SCHOOL

contact information

Postal address:

Australian Science and Mathematics School

Flinders University

Sturt Road

BEDFORD PARK SA 5042

Telephone:
+61 8 8201 5686

Facsimile:

+61 8 8201 5685

Email:
asms@flinders.edu.au

Website:

http://www.asms.sa.edu.au

South Australian Department of Education and Children's Services trading as South Australian Government Schools, CRICOS Provider Number 00018A